AMERICAN SOCIETY FOR MICROBIOLOGY | Molecular and Cellular Biology®

RESEARCH ARTICLE

GATA3 Abundance Is a Critical Determinant of T Cell Receptor β Allelic Exclusion

Chia-Jui Ku,[a] JoAnn M. Sekiguchi,[b] Bharat Panwar,[c] Yuanfang Guan,[c] Satoru Takahashi,[d] Keigyou Yoh,[d] Ivan Maillard,[a,e,f] Tomonori Hosoya,[a] James Douglas Engel[a]

Department of Cell and Developmental Biology,[a] Divisions of Molecular Medicine and Genetics[b] and Hematology-Oncology,[e] Department of Internal Medicine, Department of Computational Medicine and Bioinformatics,[c] and Life Sciences Institute,[f] University of Michigan, Ann Arbor, Michigan, USA; Department of Anatomy and Embryology, Faculty of Medicine, International Institute for Integrative Sleep Medicine (WPI-IIIS), Life Science Center, Tsukuba Advanced Research Alliance, and Laboratory Animal Resource Center, University of Tsukuba, Tsukaba, Japan[d]

ABSTRACT Allelic exclusion describes the essential immunological process by which feedback repression of sequential DNA rearrangements ensures that only one autosome expresses a functional T or B cell receptor. In wild-type mammals, approximately 60% of cells have recombined the DNA of one T cell receptor β (TCRβ) V-to-DJ-joined allele in a functional configuration, while the second allele has recombined only the DJ sequences; the other 40% of cells have recombined the V to the DJ segments on both alleles, with only one of the two alleles predicting a functional TCRβ protein. Here we report that the transgenic overexpression of GATA3 leads predominantly to biallelic TCRβ gene (*Tcrb*) recombination. We also found that wild-type immature thymocytes can be separated into distinct populations based on intracellular GATA3 expression and that GATA3^{LO} cells had almost exclusively recombined only one *Tcrb* locus (that predicted a functional receptor sequence), while GATA3^{HI} cells had uniformly recombined both *Tcrb* alleles (one predicting a functional and the other predicting a nonfunctional rearrangement). These data show that GATA3 abundance regulates the recombination propensity at the *Tcrb* locus and provide new mechanistic insight into the historic immunological conundrum for how *Tcrb* allelic exclusion is mediated.

KEYWORDS allelic exclusion, T cell receptor beta locus, GATA3, monoallelic-to-biallelic switch

One enduring mystery in cellular immunology regards the underlying mechanisms that control antigen receptor allelic exclusion (1, 2), the process whereby B or T lymphocytes are programmed to express only one functional allele for each chain of their respective antigen receptors (B cell receptor [BCR] or T cell receptor [TCR]), thus avoiding the coexistence of multiple antigen specificities in a single immune cell. Lymphocytes acquire the diversity of antigen recognition (3) as well as a unique monospecificity for particular antigens (4) during development in the bone marrow (B cells) or the thymus (T cells).

T lymphocyte development is generally characterized by division into multiple stages based on developmental timing and the location and expression of specific cell surface markers (5). T cell development begins when multipotential hematopoietic progenitor cells in the bone marrow migrate through the bloodstream to the thymus, where early T lineage progenitors (ETPs) are generated and later specified to become T cells (6–10). ETPs differentiate into double-negative (DN) cells (DN2 to DN4 stages) that express neither the CD4 nor the CD8 coreceptor, then into double-positive (DP)

Received 3 February 2017 **Returned for modification** 27 February 2017 **Accepted** 14 March 2017

Accepted manuscript posted online 20 March 2017

Citation Ku C-J, Sekiguchi JM, Panwar B, Guan Y, Takahashi S, Yoh K, Maillard I, Hosoya T, Engel JD. 2017. GATA3 abundance is a critical determinant of T cell receptor β allelic exclusion. Mol Cell Biol 37:e00052-17. https://doi.org/10.1128/MCB.00052-17.

Address correspondence to James Douglas Engel, engel@umich.edu.

($CD4^+$ $CD8^+$) cells, and finally into either CD4 single-positive (SP) helper or CD8 SP cytotoxic T cells. These naive T cells then exit the thymus and circulate to secondary lymphoid organs, where they acquire immune competence (11).

During the process of ETP differentiation into the DN2 and DN3 stages, cells become committed to the T cell lineage (12, 13) and begin to rearrange the T cell receptor β gene (*Tcrb*) (14). Rearrangement of TCRβ will finally result in the generation of a functional T cell receptor only after forming a complex with TCRα. This recombination-directed combinatorial process generates the remarkable receptor diversity observed in the $\alpha\beta$T cells that comprise 95% of adult T lymphocytes (15). The generation of functional TCRs is critical for the development of a T cell, as TCRs must specifically and sensitively recognize foreign antigens to mediate humoral immune responses (16). β-Selection is one critical step that occurs at the DN3 stage, and only cells that express a functional intracellular pre-TCR complex (containing the PTCRA [also known as pre-TCRα], CD3, and TCRβ proteins) can continue development.

At the *Tcrb* locus, the recombination events that eventually lead to the generation of a TCR complex are initiated at the ETP/DN2 stage by recombining Dβ (diversity) and Jβ (joining) DNA gene segments on both chromosomes (6). Subsequently, one of 23 functional Vβ (variable) mouse gene segments is joined to the previously rearranged DβJβ recombinant at the DN3 stage (thereby generating VDJ recombinants) to generate a *Tcrb* gene encoding the β chain of the pre-TCR complex (6, 17, 18). A similar VDJ rearrangement is also observed during B cell development at the immunoglobulin heavy chain gene (*Igh*) locus. The myriad VDJ recombination events that can be generated simply by recombinational diversity create an extraordinarily large array of TCRβ, TCRα, IgH, as well as Ig light (IgL) chains (3, 19). Any deficiency in this process can lead to increased apoptosis and severe impairment of T or B cell development, as VDJ rearrangements are required for developmental progression from progenitor to mature B and T cell stages (20, 21).

According to the clonal selection hypothesis (4), every individual T cell or B cell most often expresses only one unique TCR or BCR protein to ensure the immune specificity of that cell through a process referred to as allelic exclusion. Allelic exclusion is achieved by monoallelic V-to-DJ recombination at the *Tcrb* and *Igh* chain loci or by V-J joining at the Ig kappa (*Igk*) and Ig lambda (*Igl*) loci to ensure that two productive rearrangements cannot occur at the same time (referred to as the initiation of allelic exclusion) (22). Furthermore, a negative-feedback mechanism must also prevent further rearrangement once a productive β chain (T cells) or Ig chain (B cells) has been synthesized (i.e., yielding one productively rearranged allele and a second allele that has completed only initial DJ joining [VDJ^+/DJ]), referred to as the maintenance of allelic exclusion (23). Developing T and B cells that fail to generate functional TCRβ, IgH, or IgL proteins (because of out-of-frame DNA recombination) on the first attempt get a second chance to survive by rearrangement of the second allele that somehow becomes released from allelic exclusion. Cells that succeed after this second attempt (i.e., one allele unproductively rearranged and the other productively rearranged [VDJ^-/VDJ^+]) as well as VDJ^+/DJ cells that were productive on the first attempt can continue to differentiate and, depending on the affinity properties of these functional receptors, become mature B or T cells. Cells that fail to produce a functional receptor after both rearrangements (VDJ^-/VDJ^-) are eliminated (24). Experimentally, approximately 60% of mature T lymphocytes are of the VDJ^+/DJ genotype, while 40% are of the VDJ^-/VDJ^+ genotype (2, 24–26). The molecular mechanisms responsible for allelic exclusion remain largely unresolved (1, 2), and a deficiency in the process of allelic exclusion maintenance results in the generation of cells that express two functional TCRs, which can lead to autoimmunity (27, 28).

The transcription factor GATA3 (29, 30) has been shown to be crucial for differentiation at multiple stages of T cell development (31), including the ETP stage, the DN2 stage, the DN3-to-DN4 transition, and the CD4 stage (34, 35). The most prominent immunological event that takes place during the DN3/DN4 stage of T cell development is the recombination of the *Tcrb* loci, a process vital to the generation of T cell diversity. Mice in which *Gata3* was conditionally ablated at the DN3 stage (using an *Lck-Cre*

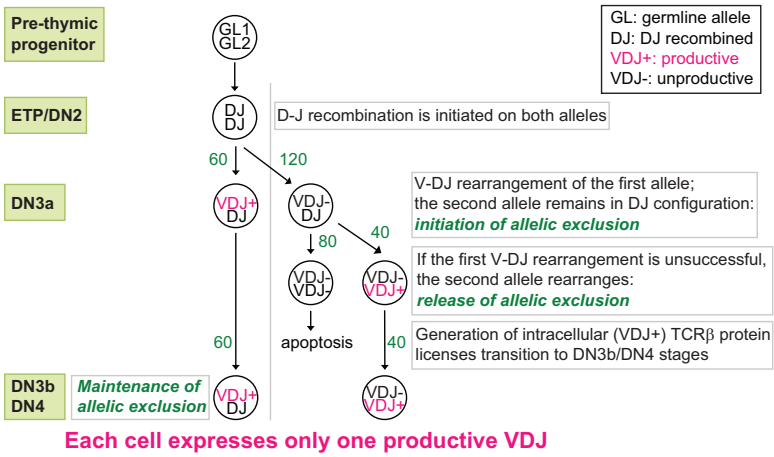

FIG 1 Regulated model for *Tcrb* VDJ rearrangement. In wild-type animals, the ratio of VDJ$^+$/DJ to VDJ$^-$/VDJ$^+$ cells is roughly 60% to 40% for both the *Igh* and *Tcrb* loci (25, 44, 45); such a regulated model as depicted here straightforwardly accounts for the actual rearrangement pattern (2). The numbers next to the arrows represent the hypothetical cell numbers that are predicted at the differentiation stage of thymopoiesis to obtain a final 60:40 ratio (2) of VDJ$^+$/DJ and VDJ$^-$/VDJ$^+$ cells that are detected in wild-type thymocytes.

transgene) had a reduced number of DN4 cells, even though those remaining DN4 cells had successfully rearranged the VDJ segments at the *Tcrb* locus (34). These data demonstrate either that GATA3 plays no role in *Tcrb* VDJ rearrangement or that an alternative pathway can partially compensate for the absence of GATA3. To date, it is unclear what role GATA3 performs at the DN3/DN4 stages when this factor is demonstrably vital for the further development of T cells (34). Here we report that the transgenic overexpression of GATA3 forfeits allelic exclusion at the *Tcrb* locus, a vital mechanism that dictates the antigen monospecificity of T lymphoid cells.

RESULTS

Transgenic overexpression of GATA3 compromises maintenance of allelic exclusion. To initially test possible functions for GATA3 in DN3 stage development (Fig. 1), we employed a transgenic line in which GATA3 was transcriptionally regulated by human *Cd2* regulatory elements (Tg$^{Cd2\text{-}GATA3}$, line 720) which is active in T and B lymphocytes but not in prethymic hematopoietic progenitors or myeloid or erythroid cells (36). We first quantified the abundance of the GATA3 protein in Tg$^{Cd2\text{-}GATA3}$ thymocytes. Western blot analysis confirmed that this transgenic line expressed an ~6-fold-greater abundance of the GATA3 protein in total Tg$^{Cd2\text{-}GATA3}$ thymocytes than in the wild type (Fig. 2A). GATA3 mRNA levels in the DN3a (151%), DN3b (180%), and DN4 (750%) stages were quantitatively higher than those in the same stages of wild-type thymocytes (Fig. 2B), as expected from the documented activity of these human *Cd2* regulatory elements (37, 38). When we quantified the stage-specific expression of the GATA3 protein by flow cytometry, we found that it was more abundant at the DN4 (245%), DP (323%), CD4 SP (167%), and CD8 SP (168%) stages than in wild-type thymocytes, but surprisingly, there was no significant difference in GATA3 abundances at the ETP, DN2, DN3a, or DN3b stage (Fig. 2C) between Tg$^{Cd2\text{-}GATA3}$ and wild-type mice; in contrast to the GATA3 mRNA abundance, no increase in the GATA3 protein concentration was observed at the DN3a/b stages (Fig. 2C) (see Discussion). No significant differences in the absolute numbers of DN3a, DN3b, or DN4 cells were observed in Tg$^{Cd2\text{-}GATA3}$ thymocytes, while modest but statistically significant increases in the numbers of DP (124%) and CD4 SP (152%) cells were observed (Fig. 2D), in agreement with the demonstrated role for GATA3 in promoting CD4 SP T cell development (34, 35).

We next investigated the global gene expression profiles in wild-type and Tg$^{Cd2\text{-}GATA3}$ mice. Thymocytes at the DN3a stage, the stage at which V-to-DJ rearrange-

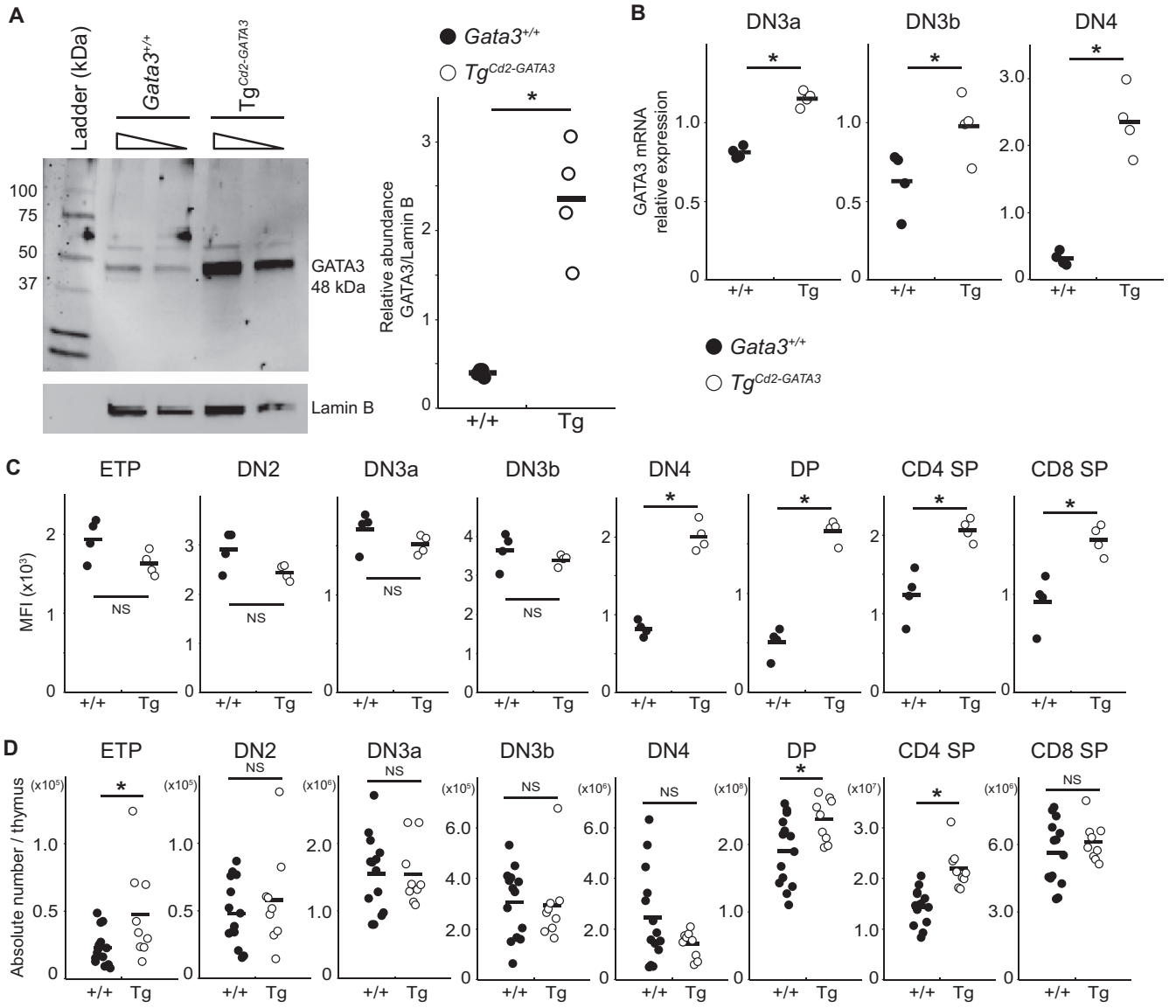

FIG 2 Forced expression of GATA3 in Tg$^{Cd2\text{-}GATA3}$ mice. (A) Western blot analysis of 10 μg or 5 μg of protein recovered from total thymocytes of a Tg$^{Cd2\text{-}GATA3}$ or wild-type (*Gata3*$^{+/+}$) mouse. The migration position of GATA3 (48 kDa) is indicated. Lamin B was used as the normalization control. A representative blot is shown; this experiment was repeated in two independent biological replicates with two mice of each genotype; results are presented graphically on the right. (B) Quantification of GATA3 mRNA levels in DN3a (Lin$^-$ cKit^{low} CD25$^+$ CD27^{low} FSC^{low}), DN3b (Lin$^-$ cKit^{low} CD25$^+$ CD27^{hi} FSC^{hi}), and DN4 (Lin$^-$ cKit$^-$ CD25$^-$) stage thymocytes isolated from Tg$^{Cd2\text{-}GATA3}$ mice or control wild-type mice by qRT-PCR. (C) Quantification of the amount of GATA3 protein by flow cytometry using the MFI (with the background intensity of IgG staining subtracted) in staged thymocytes isolated from Tg$^{Cd2\text{-}GATA3}$ mice or control wild-type mice. (D) Absolute numbers of thymocytes in mice of each genotype according to developmental stage. Each circle represents results for an individual animal. Solid bars indicate the averages for each genotype. *, $P < 0.05$; NS, not significant ($P > 0.05$).

ment takes place (39), were isolated from both Tg$^{Cd2\text{-}GATA3}$ and wild-type animals and then analyzed by transcriptome sequencing (RNA-seq). The data confirmed a modest overexpression of GATA3 mRNA (137%) in DN3a cells (Fig. 3A), as also documented by reverse transcription-quantitative PCR (qRT-PCR) (Fig. 2B). The transcript abundance of the two *Tcrb* constant regions (*Trbc1* and *Trbc2*) in Tg$^{Cd2\text{-}GATA3}$ mice was unchanged compared to that in control wild-type thymocytes (Fig. 3B). Similarly, the relative utilizations of different V region segments were indistinguishable between the Tg$^{Cd2\text{-}GATA3}$ and wild-type *Tcrb* loci (Fig. 3C). These data are compatible with normal *Tcrb* rearrangement in mice in which the *Gata3* gene was ablated at the DN3 stage using a *Lck-Cre* transgene (34).

From RNA-seq analysis, 171 genes were found to exhibit a statistically significant difference between the two genotypes (126 downregulated and 45 upregulated in Tg

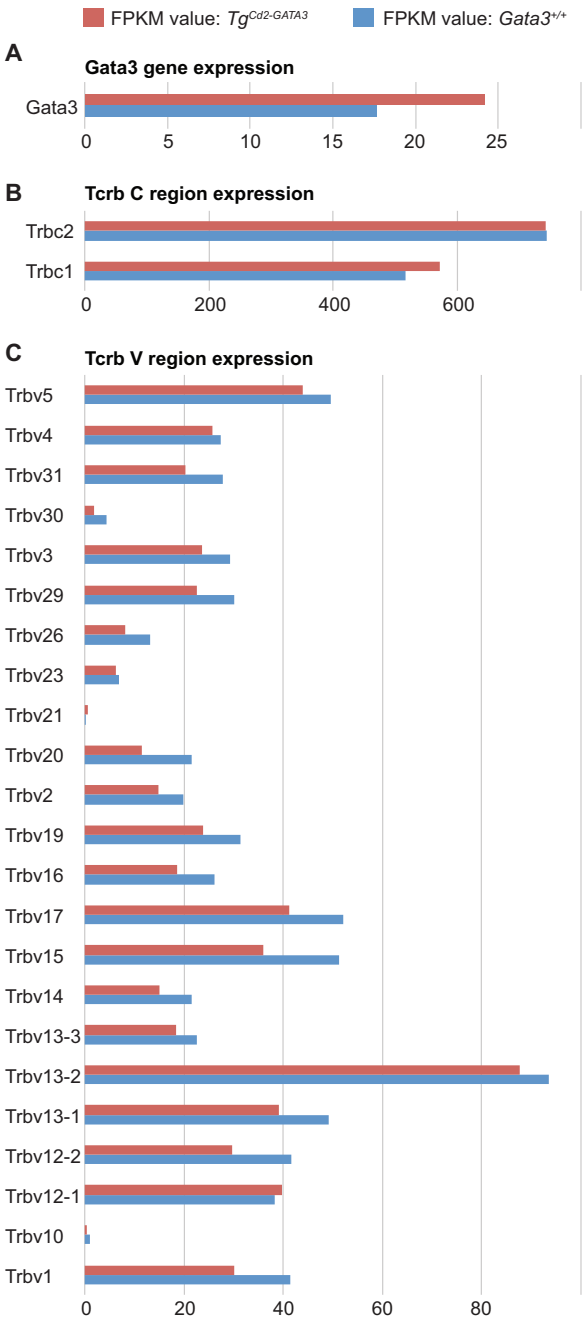

FIG 3 RNA-seq analysis of transcript abundance and V-region utilization in $Tg^{Cd2\text{-}GATA3}$ DN3a stage cells. The transcript abundances of GATA3 (A), two *Tcrb* constant regions (B), and multiple V regions (C) were quantified as fragments per kilobase per million (FPKM). None of the *Tcrb* regions showed a statistically significant difference (FDR of <0.05) between Tg and control wild-type cells.

thymocytes) (Fig. 4A). One of these genes is *Cpa3* (150% change compared to the wild type), a mast cell gene, which is also induced when excess GATA3 is retrovirally expressed in DN1/DN2 stage T cells (40) and which is downregulated by GATA3 short hairpin RNA (shRNA) knockdown of DN2 stage T cells (33). Gene ontology analysis using the DAVID functional annotation tool (41) (https://david.ncifcrf.gov/) highlighted the most significant changes in genes related to the chromosome/histone, the cell cycle, and kinetochore organization in the 126 downregulated genes (Fig. 4B). The reduced expression of many histone genes suggests changes in chromatin or replication status (Fig. 4C). These data demonstrate that a 1.5-fold increase in the GATA3 mRNA abun-

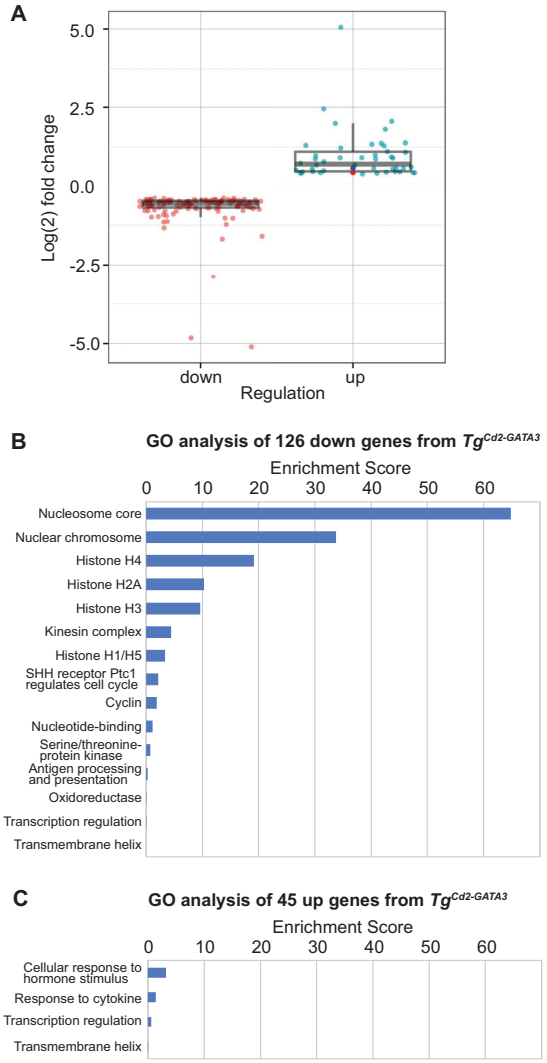

FIG 4 Gene ontology (GO) analysis of genes that exhibit statistically significant differences between $Tg^{Cd2\text{-}GATA3}$ and wild-type thymocytes. (A) From RNA-seq analysis of DN3a stage cells (conducted as described in the legend to Fig. 3), 171 genes were found to exhibit a statistically significant difference (FDR of <0.05) between the two genotypes. The 126 genes downregulated in Tg mice are shown in pink, and the 45 upregulated genes are shown in light blue. The *Cpa3* gene is highlighted in dark blue. The *Gata3* gene (highlighted in red), the abundance of which is not statistically significant (FDR = 0.249), is also shown. (B and C) Gene ontology analysis of these 126 and 45 genes was performed by using the DAVID functional annotation tool (41) (https://david.ncifcrf.gov/). The classification stringency was set to "highest."

dance at the DN3a stage of thymocyte development has no effect on *Tcrb* VDJ rearrangement initiation but results in the reduced expression of genes related to chromatin and replication status.

We next analyzed the status of *Tcrb* gene recombination by sequencing of both *Tcrb* alleles in single thymocytes using a nested two-step PCR strategy (25, 42) (see Materials and Methods). To test the reliability of this approach, we first examined the status of the *Tcrb* genes in individual wild-type DN4 stage thymocytes. DN4 stage cells, by definition, have already generated a functional TCRβ complex and have thus already passed β-selection. As summarized in Table 1, 57% of the wild-type *Gata3* DN4 stage cells are configured in a VDJ^{+}/DJ genotype configuration at the *Tcrb* loci and had productively rearranged (i.e., recombined in a DNA configuration that predicted a functional TCRβ protein) one allele while leaving the second allele in a DN2 (only DJ rearranged) state. The remaining cells (40%) were determined to be in a *Tcrb* VDJ^{-}/VDJ^{+} arrangement

TABLE 1 Genomic configuration of *Tcrb* alleles in individual DN4 stage thymocytes from wild-type or *Gata3* mutant mice

Genotype	No. (%) of cells in *Tcrb* locus genomic configuration[a]:			
	VDJ^+/DJ	VDJ^-/VDJ^+	VDJ^-/VDJ^-	VDJ^+/VDJ^+
$Gata3^{+/+}$	20/35 (57)	14/35 (40)	0	1/35 (3)
$Tg^{Cd2\text{-}GATA3}$	12/42 (29)	22/42 (52)	0	8/42 (19)
$Gata3^{g/+}$ ($eGFP^-$)	42/46 (91)	4/46 (9)	0	0
$Gata3^{g/+}$ ($eGFP^+$)	3/36 (8)	29/36 (81)	4/36 (11)	0
$Gata3^{+/+}$ ($GATA3^{LO}$)	30/32 (94)	2/32 (6)	0	0
$Gata3^{+/+}$ ($GATA3^{HI}$)	3/30 (10)	26/30 (87)	0	1/30 (3)

[a]VDJ^+/DJ cells bear one rearranged VDJ allele and one rearranged DJ allele; VDJ/VDJ cells have fully rearranged both alleles either productively or unproductively. VDJ^+ and VDJ^- indicate DNA sequencing results that predict productive and unproductive rearrangements, respectively. Data represent the summary of results from 4 to 6 animals of each genotype. Statistical analysis was performed by using Fisher's exact test, and the differences were statistically significant for all genotypes ($P = 0.0441$ between $Gata3^{+/+}$ and $Tg^{Cd2\text{-}GATA3}$; $P < 0.0001$ between $Gata3^{g/+}$ [$eGFP^-$] and $Gata3^{g/+}$ [$eGFP^+$]; $P < 0.0001$ between $Gata3^{+/+}$ [$GATA3^{LO}$] and $Gata3^{+/+}$ [$GATA3^{HI}$]).

and had therefore failed to generate a functional TCRβ protein after the first allele V-to-DJ recombination event and were successful only after recombination of the remaining unrearranged *Tcrb* locus had taken place. Very few of these wild-type DN4 thymocytes (3%; 1 out of 35 cells analyzed) predicted the generation of two functional TCRβ proteins after the recombination of both *Tcrb* alleles (43). These data confirm the anticipated frequencies of productive versus unproductive rearrangements in wild-type cells (2, 25, 44, 45) as well as the efficacy of the experimental approach.

To analyze *Tcrb* allelic exclusion, DN4 stage cells were isolated from adult $Tg^{Cd2\text{-}GATA3}$ mice, and the genomic DNA configurations of both *Tcrb* alleles were once again analyzed in single cells. Since the majority of DN3a stage cells have not completed VDJ rearrangement (39), we analyzed DN4 stage cells that had just passed β-selection. In remarkable contrast to wild-type mice, only 29% of DN4 stage cells from $Tg^{Cd2\text{-}GATA3}$ mice were in a *Tcrb* VDJ^+/DJ configuration (Table 1). Instead, the vast majority of $Tg^{Cd2\text{-}GATA3}$ DN4 thymocytes (71%) had fully recombined the variable, diversity, and joining exons of both *Tcrb* chromosomes. Importantly, we found that a highly unusual 19% of $Tg^{Cd2\text{-}GATA3}$ DN4 stage cells predicted the generation of two productively rearranged (VDJ^+/VDJ^+) *Tcrb* alleles, an extraordinarily rare occurrence in wild-type mice (Table 1) (43). These data demonstrate that an increased abundance of the GATA3 protein overrides allelic exclusion at the *Tcrb* loci in thymocytes (Fig. 5).

Since the expression of dual T cell receptors has been reported to increase autoimmunity (27, 28), we asked whether the presence of two functionally recombined *Tcrb* alleles allows T cells to present two distinct TCRβ proteins on their cell surface. To do so, we quantified the percentages of wild-type and $Tg^{Cd2\text{-}GATA3}$ T lymphocytes and splenocytes that express cell surface TCRβ chains from both alleles (46, 47). Three combinations incorporating 12 antibodies that are specific for different Vβ domains and one combination that included 4 antibodies specific for different Vα domains were used to monitor biallelic TCR expression on αβ T cells isolated from the thymi and spleens of wild-type and $Tg^{Cd2\text{-}GATA3}$ animals. A significantly increased frequency of dual-TCRβ-expressing $CD3^+$ T cells in $Tg^{Cd2\text{-}GATA3}$ thymi (Fig. 6) confirmed the conclusion that enforced GATA3 expression surmounts normal *Tcrb* allelic exclusion. However, the frequencies of dual-TCRβ-expressing $CD3^+$ T cells were equivalent in $Tg^{Cd2\text{-}GATA3}$ and wild-type splenocytes (Fig. 6), suggesting that cells expressing two surface TCRβ receptors survive thymopoiesis but are eliminated before or during exposure to splenic maturation. These data show that even when the genetic programs that normally regulate TCRβ expression are compromised (for example) by forced GATA3 overexpression, later cellular homeostatic control over "phenotypic" allelic exclusion (2, 48) is still maintained.

The maintenance of *Tcrb* allelic exclusion coincides with the repression of one *Gata3* allele. Since the *Gata3* monoallelic-to-biallelic transcriptional switch (49) is first

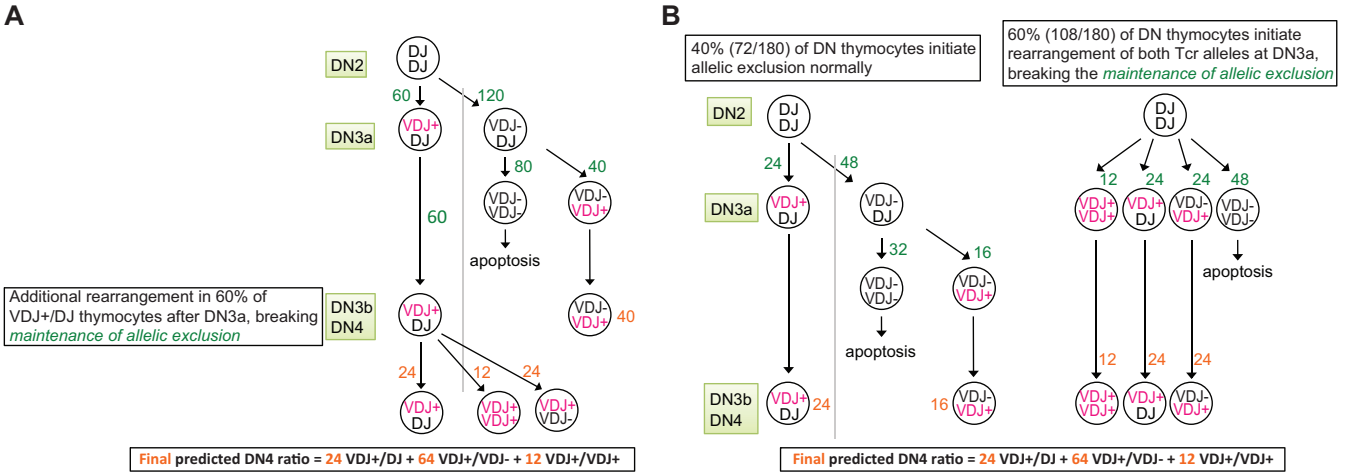

FIG 5 *Tcrb* VDJ rearrangement in mice that express superabundant GATA3. The numbers (green) next to each of the arrows represent the hypothetical cell numbers that would be predicted, under various conditions (bottom), at each developmental stage to obtain 100 surviving cells (shown in orange) after completion of thymic development. In marked contrast to wild-type mice, only 29% of DN4 stage thymocytes in $Tg^{Cd2\text{-}GATA3}$ mice were of the *Tcrb* VDJ^{+}/DJ genotype (Table 1). Instead, the vast majority of $Tg^{Cd2\text{-}GATA3}$ DN4 stage cells (71%) had fully recombined (VDJ/VDJ) both *Tcrb* alleles. Importantly, we found that an extraordinary 19% of $Tg^{Cd2\text{-}GATA3}$ DN4 stage cells bore DNA sequences that predicted two productively rearranged (VDJ^{+}/VDJ^{+}) *Tcrb* alleles, which is extremely rarely observed in wild-type mice (43). (A) One possible explanation (model 1) for the unexpected frequencies of DN4 *Tcrb* rearrangements in enforced GATA3 transgenic mice is that allelic exclusion is normal at the *Tcrb* loci at the DN3 stage (when the GATA3 protein abundance is normal, at 91% and 93% of the wild-type levels at the DN3a and DN3b stages, respectively), but later, at the DN4 stage, when the level of the GATA3 protein has increased (245% of the wild-type level) (Fig. 2C), the maintenance of allelic exclusion is forfeit in 50 to 70% of T cells, and the *Tcrb* genomic DNA now undergoes V-to-DJ rearrangement at the DN3b or DN4 stage, which has not been previously reported to occur in wild-type mice. (B) Alternative model (model 2). The human *Cd2* regulatory sequences are active in DN1 (~50%)-, DN2 (~50%)-, DN3 (~99%)-, DN4 (~98%)-, and later-stage T cells based on an analysis of hCD2-GFP transgenic mice (38). In accord with those observations, we observed excess expression of GATA3 mRNA in $Tg^{Cd2\text{-}GATA3}$ mice at the DN3a (151%) and DN3b (180%) stages compared to wild-type thymocytes (Fig. 2B). The abundance of the GATA3 protein in $Tg^{Cd2\text{-}GATA3}$ mice increased by the DN4 stage, but a similar increase was not detectable at the DN3a or DN3b stage, when measured by the MFI of intracellular GATA3 staining (Fig. 2C). Therefore, we cannot exclude the possibility that a GATA3 mRNA-dependent mechanism compromises the initiation of allelic exclusion in 50 to 70% of DN3a cells (right) to generate VDJ^{+}/VDJ^{+} cells in $Tg^{Cd2\text{-}GATA3}$ mice. In either model, the excess expression of GATA3 predicts compromised allelic exclusion at the DN3a or DN4 stage. This altered regulatory potential of GATA3 supports the hypothesis that increased GATA3 expression partially caused by the *Gata3* monoallelic-to-biallelic switch releases the second *Tcrb* locus from allelic exclusion (Fig. 1).

observed at around the same developmental stage (DN2/DN3) as when the *Tcrb* loci initiate VDJ genomic DNA rearrangement, we hypothesized that *Gata3* monoallelic expression might be functionally associated with allelic exclusion at the *Tcrb* locus.

We previously generated a GATA3-enhanced green fluorescent protein (eGFP) fusion protein knock-in allele ($Gata3^{g}$) by embryonic stem (ES) cell gene targeting (32, 50), and by both RNA-fluorescence *in situ* hybridization (FISH) and RT-PCR single nucleotide variant (SNV) sequencing of single thymocytes, we recently demonstrated that a *Gata3* monoallelic-to-biallelic transcriptional switch initiates at around the DN2 stage (49). In concert with those observations, hypomorphic $Gata3^{g/g}$ homozygous thymocytes were shown to exhibit a second peak of GFP fluorescence starting at the DN2 stage in thymocytes that were generated after adoptive transfer of fetal liver hematopoietic stem cells (HSC) and progenitors (see Fig. 3 in reference 49) ($Gata3^{g/g}$ mutants could not be examined directly since the homozygous mutation leads to perinatal lethality [50]). In initially curious contrast, GFP fluorescence was never observed at the ETP, DN2, or DN3 stage in $Gata3^{g/+}$ heterozygous mutants (32, 49). We then hypothesized that this apparent contradiction might be explained by the facts that the $Gata3^{g}$ allele is a hypomorph and that its reduced activity, if expressed in ETPs (where *Gata3* is monoallelic), would not be adequate to allow these cells to survive, while ETPs that initially express the wild-type ($Gata3^{+}$) allele should be able to developmentally progress in a normal fashion.

At the DN4 stage, approximately half of the T cells express both the hypomorphic ($Gata3^{g}$) and wild-type ($Gata3^{+}$) alleles, while half continue to express only the $Gata3^{+}$ allele (and remain nonfluorescent) in $Gata3^{g/+}$ heterozygous mice (49). The expression levels of GATA3 mRNA and protein in nonfluorescent (eGFP-negative [$eGFP^{-}$]) DN4 cells of $Gata3^{g/+}$ heterozygous mutant mice support the concept that the $eGFP^{-}$ cells

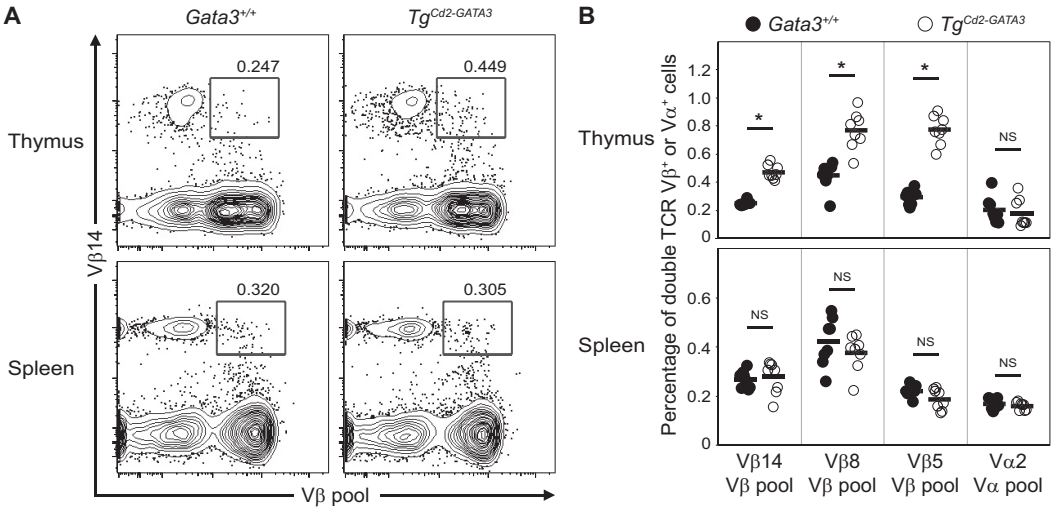

FIG 6 Dual-TCRβ thymocytes are abundant in the thymi but not the spleens of $Tg^{Cd2\text{-}GATA3}$ mice. (A) Representative flow cytometric analysis of Vβ14 (ordinate axis) versus a pool containing 11 different anti-Vβ antibodies (abscissa) (anti-Vβ2, -4, -5.1/5.2, -6, -7, -8, -9, -10b, -11, -12, and -13) from $CD3^+$ thymocytes (top) or splenocytes (bottom) isolated from wild-type ($Gata3^{+/+}$) (left) or $Tg^{Cd2\text{-}GATA3}$ (right) animals. The percentages of cells expressing two different cell surface TCR $V\beta^+$ complexes are shown in the insets. (B) Graphical summary of the frequencies of $CD3^+$ thymocytes and splenocytes from wild-type ($Gata3^{+/+}$) and $Tg^{Cd2\text{-}GATA3}$ mice that express the indicated combinations of TCR Vβ (anti-Vβ14, -Vβ8, and -Vβ5.1/5.2 versus the Vβ pool containing anti-Vβ2, -4, -5.1/5.2, -6, -7, -8, -9, -10b, -11, -12, and -13; note that Vβ8 and Vβ5.1/5.2 were not included in the Vβ pool when Vβ8 and Vβ5.1/5.2 were used for individual staining, respectively) and Vα (anti-Vα2 versus the Vα pool, including anti-Vα3.2, -8.3, and -11.1/11.2) (see Table 3 for details on antibodies used). Each circle represents results for an individual animal from two independent experiments for a total of eight mice. The horizontal bar for each group indicates the average frequency. *, $P < 0.05$; NS, not significant.

express only the wild-type allele, and the more abundant expression of the GATA3 protein in fluorescent than in nonfluorescent $Gata3^{g/+}$ DN4 stage thymocytes supports the inference that fluorescent cells express this transcription factor from both alleles (see Fig. S6 and S7 in the supplemental material in reference 49).

To test the hypothesis that *Gata3* monoallelic repression correlates with *Tcrb* allelic exclusion, we purified both $eGFP^-$ (nonfluorescent *Gata3* monoallelic) and eGFP-positive ($eGFP^+$) (fluorescent biallelic) DN4 stage thymocytes (Fig. 7A). We then analyzed the VDJ rearrangement status of both *Tcrb* loci in individual cells as described above. When we examined the recombination status of the *Tcrb* loci in individual DN4 $Gata3^{g/+}$ nonfluorescent cells (where only the wild-type allele is expressed) or $eGFP^+$ cells (in which both wild-type and "g" alleles are expressed), we found that 91% of nonfluorescent DN4 stage cells were in a VDJ^+/DJ configuration (Table 1), which differs dramatically from the frequency observed in wild-type thymocytes. In stark contrast, 81% of the DN4 stage $eGFP^+$ cells (in which both *Gata3* alleles are transcribed) were in a VDJ^-/VDJ^+ configuration (Table 1). (Interestingly, we also recovered 11% fluorescent DN4 cells that had unproductively rearranged both *Tcrb* alleles [VDJ^-/VDJ^-]; we speculate that these cells probably represent thymocytes that had not yet been eliminated normally by apoptosis.) Taken together, these data demonstrate that developing T cells in which allelic exclusion is maintained at the *Tcrb* locus bear one repressed and one active *Gata3* allele, while thymocytes in which both *Tcrb* loci have been fully (either productively or unproductively) rearranged transcribe *Gata3* almost invariably from both alleles.

Endogenous GATA3 abundance correlates with *Tcrb* allelic exclusion in wild-type thymocytes. To test whether the observed correlation between *Tcrb* allelic exclusion and *Gata3* expression might be an artifact that was somehow generated by employing the hypomorphic mutant $Gata3^g$ allele, we next examined wild-type mice. When the intracellular GATA3 protein abundance was analyzed at all T cell developmental stages by flow cytometry, quite remarkably, two distinct populations were reproducibly observed at the DN4 but not at the ETP, DN2, or DN3 stage in wild-type

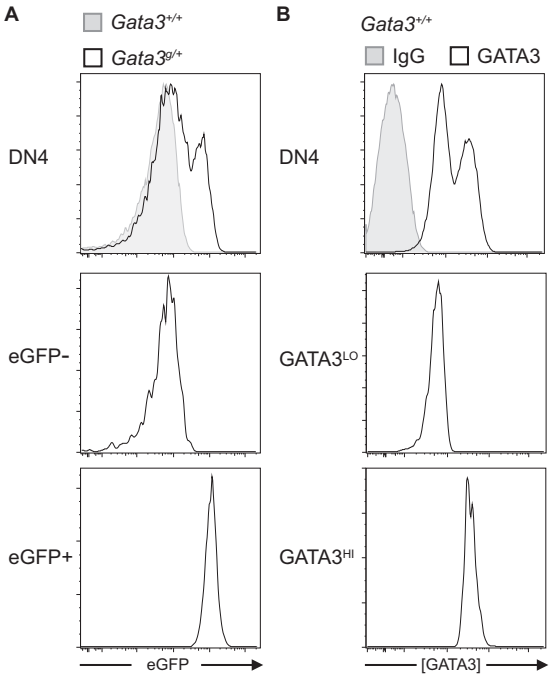

FIG 7 Wild-type and mutant DN4 stage thymocytes can be separated into two distinct pools based on the relative abundance of GATA3 expression. (A) *Gata3*$^{g/+}$ DN4 stage thymocytes can be resolved into two distinct populations, one that does not express GFP and one that does (49), compared to DN4 stage thymocytes from *Gata3*$^{+/+}$ mice. The middle and bottom panels depict the expression of the eGFP^{-} and eGFP^{+} populations after resorting. (B) GATA3^{HI} and GATA3^{LO} DN4 stage populations in wild-type mice. Thymocytes isolated from wild-type mice were stained to identify DN4 stage-specific cell surface markers and then fixed for intracellular GATA3 staining or the IgG background. Total DN4-gated cells are shown at the top, and separate GATA3^{HI} and GATA3^{LO} flow-sorted cells (middle and bottom) were then reanalyzed by flow cytometry. A representative histogram is shown; this pattern is gender independent and was reproducible in at least 10 wild-type animals in five independent experiments (see Fig. 8C).

thymocytes but were never observed at any stage in Tg$^{Cd2\text{-}GATA3}$ thymocytes (Fig. 8A and B and see Discussion). Since the abundance indicated by the staining of both populations at the DN4 stage was greater than IgG background control fluorescence (Fig. 7B and 8B and C), these wild-type cells must represent two distinct populations expressing either more (GATA3^{HI}) or less (GATA3^{LO}) abundant GATA3, while the mean fluorescence intensity (MFI) in GATA3^{HI} cells was approximately 5-fold higher than that in GATA3^{LO} cells (Fig. 8D). This frequency was in agreement with our previous observations that approximately half of DN4 stage T cells express monoallelic *Gata3* (GATA3^{LO}) and that half express both alleles (biallelic; GATA3^{HI}) at the DN4 and later stages (49).

Given the fact that we could readily separate wild-type DN4 stage thymocytes into pools harboring either more or less abundant GATA3 protein, by using the strategy described above, we analyzed the genomic DNA configurations at the *Tcrb* loci in single, fixed, wild-type DN4 stage cells representing the GATA3^{HI} or GATA3^{LO} population (Fig. 7B). As anticipated, 94% of GATA3^{LO} DN4 stage cells were of the *Tcrb* VDJ^{+}/DJ genotype, while 87% of GATA3^{HI} DN4 stage cells were of the VDJ^{-}/VDJ^{+} genotype (Table 1). Note that there was 1 cell out of the 30 cells analyzed that was in a VDJ^{+}/VDJ^{+} configuration, which is observed only rarely in nature (43) but is consistent with a very infrequent chance of recovery in randomly analyzed wild-type DN4 thymocytes (Table 1). Taken together, these observations suggest a model in which the GATA3 abundance must be quite precisely controlled to ensure that allelic exclusion is properly executed at the *Tcrb* locus and suggest that an alteration of the GATA3 abundance can lead to changes in T cell phenotypes.

Hierarchy of the *Gata3* monoallelic-to-biallelic switch and release from *Tcrb* allelic exclusion. We found that release from allelic exclusion was almost exclusively

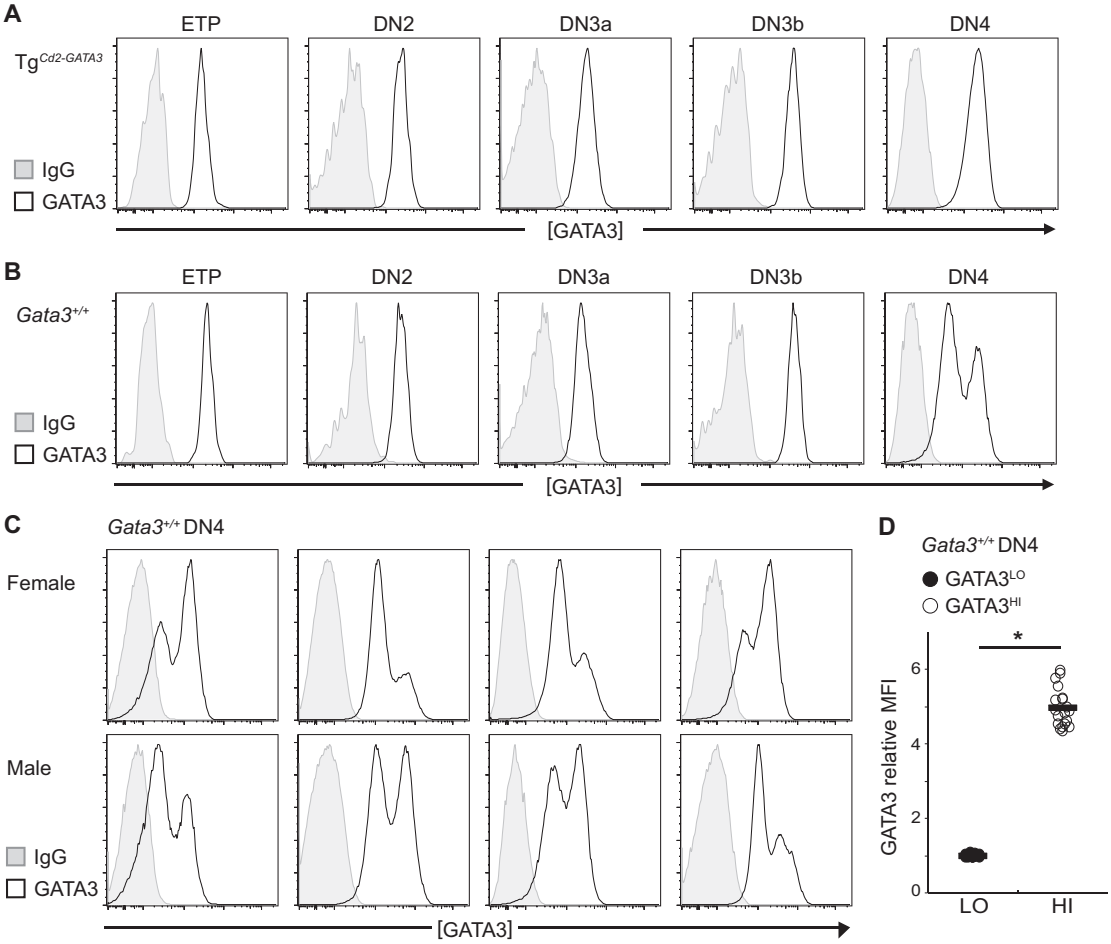

FIG 8 Profiles of GATA3 in wild-type and mutant cells. (A and B) Representative histograms of intracellular GATA3 protein abundance analyzed by flow cytometry in ETP, DN2, DN3a, DN3b, and DN4 stage thymocytes isolated from 5- to 8-week-old $Tg^{Cd2\text{-}GATA3}$ mice (A) and wild-type ($Gata3^{+/+}$) mice (B). Thymocytes were first stained for the cell surface markers used to distinguish between the various early developmental T cell stages (Materials and Methods) and then fixed and stained for intracellular GATA3 or IgG. (C) Gender-independent GATA3 protein expression in DN4 stage cells. Shown are intracellular GATA3 protein abundances in DN4 stage thymocytes from female (top) or male (bottom) wild-type animals. Eight individual animals were analyzed in seven independent experiments. (D) Quantification of GATA3 protein abundance in wild-type DN4 stage cells by flow cytometry as described above for panel C. The relative abundance of GATA3 was calculated based on the MFI of the $GATA3^{HI}$ population normalized to the $GATA3^{LO}$ population to eliminate the fluorescence intensity alteration due to flow cytometry settings that differ in independent experiments. Each circle represents results for an individual animal. Solid bars indicate the averages for each genotype. *, $P < 0.05$.

restricted to $GATA3^{HI}$ DN4 stage cells (Table 1). The *Gata3* monoallelic-to-biallelic transcriptional switch is first observed in approximately 30% of DN2 stage cells (49), while D-to-J joining is observed at the *Tcrb* loci at the ETP/DN2 stages, and V-to-DJ rearrangement takes place only at the next stage, the DN3a stage (6, 39). This observation argues logically that the *Gata3* monoallelic-to-biallelic switch is not initiated by the pre-TCR signaling pathway, which is operative only after the DN3 stage and which triggers release from allelic exclusion (25, 51). To directly test the deductive conclusion that the release from *Tcrb* allelic exclusion plays no role in the *Gata3* monoallelic-to-biallelic switch, we crossed TCRβ C57BL/6J transgenic mice, which express a functionally rearranged TCRβ transgene (52, 53), with wild-type FVB/NJ mice. In these animals, all T cells express a functional TCRβ protein under the control of native *Tcrb* gene regulatory elements, and therefore, no T cell initiates rearrangement of the endogenous *Tcrb* loci (51). We isolated developmentally staged T cells and analyzed mono- or biallelic expression of *Gata3* by single-cell RT-PCR followed by sequencing over the silent coding sequence SNV that differs in C57BL/6J and FVB/NJ mice (49). The *Gata3* monoallelic-to-biallelic switch was first observed at the DN2 stage in approximately 30

TABLE 2 Summary of mono- and biallelic GATA3 mRNA expression in single, staged adult thymocytes (GATA3 RT-PCR SNV sequence) in TCRα TCRβ or TCRβ transgenic mice[a]

Mouse and developmental stage	No. of cells with monoallelic expression		No. of cells with biallelic expression	% of cells with monoallelic expression
	Paternal	Maternal		
$Tg^{TCR\alpha TCR\beta}$				
ETP	10	11	1	95
DN2	14	11	11	69
DN3a	8	8	2	89
DN3b	9	8	13	57
DN4	11	6	13	57
$Tg^{TCR\beta}$				
ETP	17	7	4	86
DN2	10	7	25	42
DN3a	8	8	26	39
DN3b	8	5	29	31
DN4	16	10	16	62

[a]Data represent a summary of results from 3 or 4 animals analyzed at each stage.

to 50% of cells and reached approximately 50% of cells by the DN3b stage in TCRβ transgenic mice (Table 2), as also observed for wild-type thymocytes (49). These data demonstrate that the *Gata3* monoallelic-to-biallelic switch is initiated independently of release from *Tcrb* allelic exclusion.

Dissecting the molecular mechanism by which GATA3 regulates allelic exclusion. To address the detailed mechanism by which GATA3 regulates allelic exclusion, we initially examined the expression of several other genes that have been shown to be directly or indirectly involved in VDJ rearrangement. To do so, DN3a, DN3b, and DN4 stage thymocytes were isolated from $Tg^{Cd2\text{-}GATA3}$ or wild-type mice by flow sorting and then analyzed by qRT-PCR (Fig. 9). Only a few molecules have previously been shown to affect allelic exclusion, and therefore, we asked whether or not the expression of any

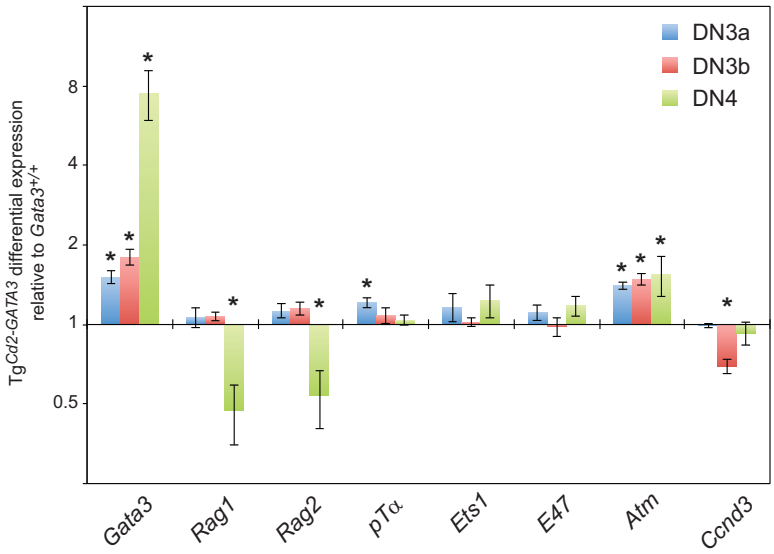

FIG 9 Relative expression levels of genes known to affect *Tcrb* allelic exclusion. Shown are data from qRT-PCR analysis of genes related to VDJ rearrangement and allelic exclusion at the *Tcrb* locus in DN3a, DN3b, and DN4 stage thymocytes isolated from $Tg^{Cd2\text{-}GATA3}$ and control wild-type mice at 5 to 8 weeks of age. The mRNA expression levels were normalized to the values for beta-actin at each stage. The fold change relative to the wild type (set at 1) at each stage is shown. GATA3 expression represents total GATA3 transcripts regulated by *hCd2* regulatory sequences plus endogenous GATA3 (same as shown in Fig. 2B). The data summarize the results of analyses of four mice of each genotype from two independent experiments. *, $P < 0.05$.

of them was significantly altered in staged thymocytes from wild-type or $Tg^{Cd2\text{-}GATA3}$ mice.

Rag1 and *Rag2* (54) are specifically suppressed at the DN4 stage in *Gata3* transgenic thymocytes but not in DN3a or DN3b stage cells (Fig. 9), and therefore, it seems unlikely that GATA3 might promote VDJ rearrangement by enhancing RAG1 and RAG2 expression. PTCRA (pTα) forms a developmentally required intracellular pre-TCR complex with the TCRβ protein that is finally translated from functionally rearranged *Tcrb* loci in DN3 cells, and *Ptcra*-null mutant mice generate a higher frequency of thymocytes bearing two productively rearranged TCRβ alleles (25), similar to the phenotype observed here for $Tg^{Cd2\text{-}GATA3}$ thymocytes (Table 1). Another important insight arose from the early observation that the enforced transgenic expression of a functional TCRβ protein represses the rearrangement of the endogenous *Tcrb* genes (51), strongly implying that a signal from the pre-TCR complex is required to maintain allelic exclusion at the *Tcrb* locus. The transcription factor ETS1 has also been shown to play an important functional role downstream of the pre-TCR signaling complex to ensure that allelic exclusion is maintained as well as for the differentiation of DN3a cells to the DN3b stage (46), but how it does so has not been clarified further. Forced E47 expression has also been shown to antagonize pre-TCR-mediated feedback signaling to thereby alter allelic exclusion (55). The cell cycle regulatory proteins ATM and cyclin D3 (CCND3) cooperate to enforce allelic exclusion at both the *Igh* and *Tcrb* loci (47). When each of these established effectors of allelic exclusion was individually analyzed by qRT-PCR in wild-type and $Tg^{Cd2\text{-}GATA3}$ thymocytes, they all exhibited a $<$2-fold change in mRNA abundance in DN3a, DN3b, or DN4 stage cells (Fig. 9). Therefore, it seems most prudent to tentatively conclude that GATA3 regulates allelic exclusion at the *Tcrb* loci through novel pathways that are independent of all of those factors that have been reported previously.

DISCUSSION

Allelic exclusion is a universal immunological feedback mechanism by which only one autosomal allele encoding antigen receptors is permitted functionality at any given time: rearrangement of the second allele of these genes is allowed only when the first rearrangement (or after somatic editing in B cells [56]) yields a defective protein. Here we provide evidence that an elevated GATA3 protein concentration promotes excessive VDJ recombination at the *Tcrb* loci, superseding allelic exclusion. Single-cell analyses of thymocytes isolated from transgenic mice that express excess (over normal abundance) GATA3 demonstrated the capacity for GATA3 to dramatically influence allelic exclusion at the *Tcrb* locus. We found that in wild-type mice, the majority of the two *Tcrb* chromosomes in $GATA3^{LO}$ DN4 (post-β-selection) stage thymocytes are arranged in a VDJ^{+}/DJ configuration, while the overwhelming majority of $GATA3^{HI}$ DN4 stage cells had fully recombined both *Tcrb* loci. Based on these data, we conclude that the GATA3 abundance plays a critical role in ensuring that allelic exclusion is properly executed at the *Tcrb* loci and that alterations in the GATA3 abundance lead to predictable changes in T cell phenotypes (Fig. 10).

GATA3 is required for the progression of T cells through multiple thymocyte developmental stages, including the transition from the DN3 stage to the DN4 stage (31). Development from DN3 to DN4 stage thymocytes was blocked in adult mice that were conditionally ablated for *Gata3* at the DN3 stage using an *Lck-Cre* transgene to inactivate $Gata3^{flox/flox}$ (34) as well as in adoptively transferred animals that were reconstituted with homozygous hypomorphic mutant $Gata3^{g/g}$ fetal liver HSC and progenitors (32). Here we show that an elevated GATA3 abundance leads to a forfeiture of *Tcrb* allelic exclusion by analyzing the recombination status of both *Tcrb* alleles in single thymocytes recovered from both $Tg^{Cd2\text{-}GATA3}$ and wild-type mice. Previous studies showed that GATA3 must be expressed to pass from the DN3 stage to the DN4 stage (34), but we also demonstrate that its abundance must be tightly regulated in order to maintain allelic exclusion at the *Tcrb* locus.

Curiously, and in contrast to observations for the DN4 stage, we did not detect two

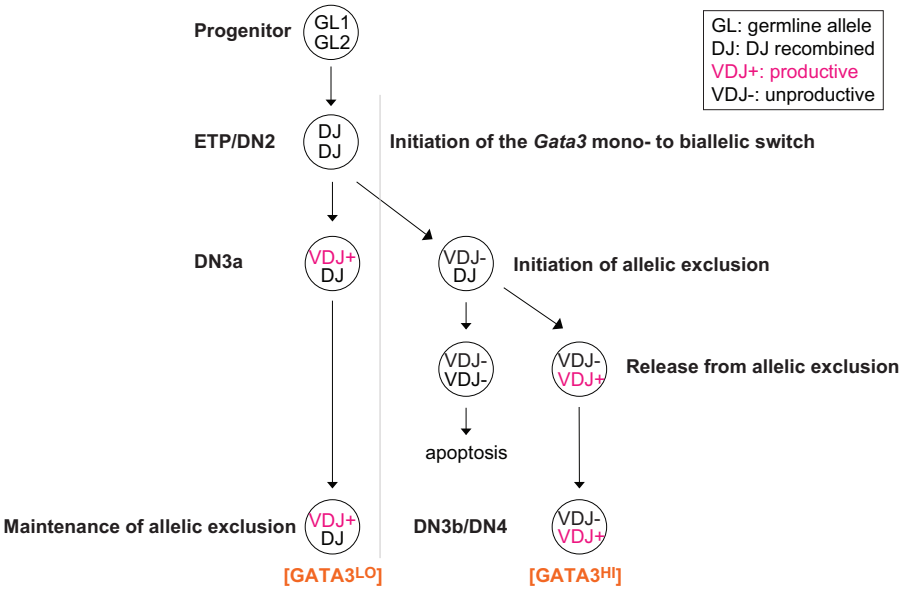

FIG 10 Model for how altered GATA3 abundance regulates *Tcrb* VDJ rearrangement. The illustration summarizes how the GATA3 abundance might modulate *Tcrb* VDJ rearrangement: while approximately 90% of DN4 stage T cells that express less GATA3 (monoallelic *Gata3* cells) bear a *Tcrb* VDJ^{+}/DJ genotype, reciprocally, approximately 90% of DN4 stage cells that express higher levels of GATA3 (biallelic *Gata3* cells) have rearranged both *Tcrb* alleles (Table 1). This led to the hypothesis that the GATA3 abundance must be quite precisely regulated in order to maintain allelic exclusion at the *Tcrb* locus and further suggested that the increase in the GATA3 abundance resulting at least partially from the *Gata3* monoallelic-to-biallelic transcriptional switch might be responsible for the release of the second (only DJ rearranged) *Tcrb* locus from allelic exclusion.

fluorescence peaks that would be indicative of an increased GATA3 abundance in wild-type thymocytes at the DN2 or DN3 stage (when *Gata3* biallelic transcription is first detected) (Fig. 8B) (49). Possible explanations for this seemingly contradictory behavior are that (i) the change in the GATA3 protein abundance is lower than the detection limit by flow cytometry at these stages, (ii) the GATA3 protein abundance may lag behind its transcriptional activity (since the transcription of *Gata3* must be followed by splicing, nuclear export, translation, posttranslational modification, and nuclear relocalization), (iii) there may be a presently cryptic mechanism that regulates the homeostatic intracellular concentration of the GATA3 protein in DN2 and DN3 stage cells, or (iv) a transient elevation of the GATA3 level could be masked by the rapid differentiation of DN3a stage cells into DN3b (and on to DN4) stage cells immediately after successful rearrangement. Similarly, an increase in the GATA3 protein level at these stages was not observed in Tg$^{Cd2\text{-}GATA3}$ mice (Fig. 2C), while the GATA3 mRNA level was clearly increased (Fig. 2B). Furthermore, when we quantified the GATA3 protein abundance by intracellular staining with an anti-GATA3 antibody followed by flow cytometry, only a single peak was observed in Tg$^{Cd2\text{-}GATA3}$ DN4 stage cells (Fig. 8A), while two peaks were always detected in wild-type animals (Fig. 8B). Importantly, the MFI of the intracellular GATA3 signal in Tg$^{Cd2\text{-}GATA3}$ mice was essentially equivalent to that in the GATA3^{HI} peak in wild-type thymocytes. According to data from reporter transgene analyses, the human *Cd2* regulatory elements are active in almost 100% of DN3/DN4 stage cells (38). One possible explanation for the failure to detect GATA3^{HI+} DN4 stage cells (GATA3^{HI} plus transgenic GATA3) is that these cells cannot survive. An alternative explanation is that a presently undefined posttranslational mechanism regulates the abundance of the GATA3 protein to prevent excessive abundance above the level expressed in GATA3^{HI} thymocytes. In addition to mono- or biallelic transcription, GATA3 autoregulation may contribute to achieving the observed 5-fold-higher GATA3 protein abundance in the GATA3^{HI} population than in GATA3^{LO} cells. Importantly, when we quantified the GATA3 abundance according to the MFI of intracellular GATA3 in

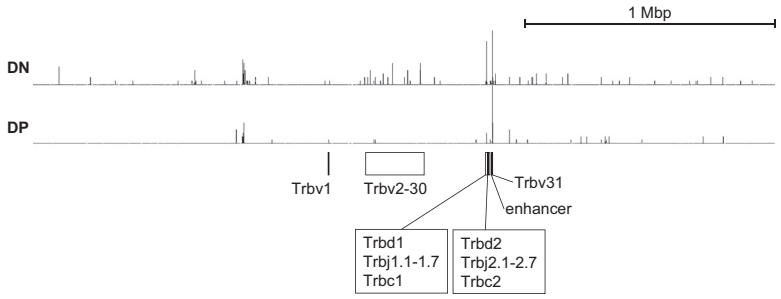

FIG 11 GATA3 binding in the *Tcrb* locus. Short-read data (Sequence Read Archive [SRA] files) of GATA3 ChIP-seq experiments performed on DN and DP stage thymocytes (GEO accession number GSE20898) (58) were obtained from the public GEO database. The raw reads were aligned to mouse genome build mm10 by using DNASTAR software to generate wig files. The wig files were loaded into Integrated Genome Browser software version 9.0.0 (http://bioviz.org/igb/). The genome region around the *Tcrb* locus (chromosome 6, positions 39700001 to 42700000) is shown. *y* axis scales are set by value (minimum of 5 and maximum of 22) for both DN and DP data. The positions of the V, D, J, and C regions of the *Tcrb* gene as well as its enhancer (83) are depicted at the bottom.

flow-sorted DN4 stage fluorescent and nonfluorescent cells recovered from *Gata3*$^{g/+}$ thymi, the apparent concentration of GATA3 was approximately 3-fold higher in fluorescent biallelic DN4 stage cells than in nonfluorescent monoallelic cells (see Fig. S6B in the supplemental material in reference 49). Taken together with the data shown in Table 1 and the 245% increase in the GATA3 abundance in Tg$^{Cd2\text{-}GATA3}$ DN4 cells, as little as a 2.5-fold increase in the GATA3 concentration appears to be sufficient to override the maintenance of allelic exclusion at the *Tcrb* loci in thymocytes.

A mechanism describing how the expression of more abundant GATA3 quashes the maintenance of allelic exclusion at the *Tcrb* locus remains incompletely resolved. Since no genes that were previously reported to be involved in *Tcrb* allelic exclusion exhibited significant differences in mRNA expression levels (Fig. 9), we conclude that GATA3 probably regulates allelic exclusion through novel pathways, with one likely possibility being that a presently undefined transcriptional target of GATA3 directly promotes *Tcrb* rearrangement. GATA3 binds to the (A/T)GATAA sequence (29, 57, 58) in chromatin, and while not ubiquitously expressed, GATA3 has been shown to function as either a transcriptional activator or a repressor in many different tissues and cell types (29, 30, 59–63). A second viable hypothesis is that GATA3 directly controls the accessibility or nuclear localization of the *Tcrb* loci in chromatin (64), and it is this feature of the nuclear architecture that is regulated in the GATA3 pathway. Computationally, more than 10 high-affinity binding sites for GATA3 have been identified (by chromatin immunoprecipitation sequencing [ChIP-seq]) within the *Tcrb* locus (58) (Fig. 11), in support of the latter model. Although no report has shown that GATA3 functions in a manner other than as a classical DNA binding transcription factor (as does, for example, Scl/Tal1 [65] or the aryl hydrocarbon nuclear translocator [66]), such a binary function for GATA3 cannot be excluded.

While the present data clearly demonstrate that an increased GATA3 abundance promotes release from mechanisms that normally regulate allelic exclusion, we note that even in the complete absence of GATA3, VDJ rearrangement at the *Tcrb* locus still takes place (34). This study implies that there must be an additional GATA3-independent mechanism(s) that promotes VDJ rearrangement, and we are currently investigating the hypothesis that a GATA3-independent mechanism is responsible for VDJ rearrangement in the absence of GATA3. Such a factor contributing to this hypothetical alternative mechanism might result in induced mRNA or protein expression or have a changed intracellular localization in *Gata3* mutant thymocytes. An alternative model that was previously suggested for T cell development is that no factor shows any change in expression levels, but the second *Tcrb* VDJ rearrangement can still be achieved, only much slower than the speed at which the process progresses in the presence of normal levels of GATA3.

We and many others previously demonstrated that the abundance of a transcription factor can be a critical determinant for the execution of its biological function. Proplatelet formation is inhibited after either diminished or excessive expression of the transcription factor MafG in megakaryocytes (67), and T cell development in the thymus is blocked when there is either too little or too much GATA3 (32, 33, 40, 68, 69). Of note in this regard, the inactivation of one *Gata3* allele often results in a mild reduction in T cell development in humans (HDR [hypoparathyroidism, deafness, and renal dysplasia] syndrome) (70–72) and in mice (49), while a 2-fold increase in the GATA3 protein abundance has been shown to induce T cell lymphoma (73). Here we show that a 2.5- to 5-fold increase in the GATA3 abundance (calculated from the fluorescence intensity), caused at least in part by monoallelic-to-biallelic *Gata3* transcriptional activation, regulates allelic exclusion at the *Tcrb* locus. These data emphasize the importance of gene regulation at the transcriptional level: it is by now axiomatic that the tissue specificity, the timing of expression, as well as the absolute abundance of a transcription factor can each play a critical role in ultimately determining pathophysiology.

In summary, we report here that the GATA3 concentration is a principal determinant of allelic exclusion at the *Tcrb* locus. The next goals in further detailing the mechanisms delineating this process are to investigate the independent gene targets that GATA3 activates (and represses) to elicit its independent requirement for T cell development beyond the DN3 stage and for breaking the maintenance of allelic exclusion. Another immediate goal will be to determine how *Gata3* transcription itself is so precisely controlled and how the second allele is released from repression in a specific subset of DN2/3 stage cells. Finally, it is of considerable interest to contemplate whether or not the conceptually parallel process of IgH BCR recombination is subject to a similar regulation and what the identity of the regulatory proteins that execute the analogous process in B lymphocytes might be.

MATERIALS AND METHODS

Mice. *Gata3*^{g} (32, 50), GATA3 Tg$^{Cd2\text{-}GATA3}$ transgenic line 720 (36), TCR$\alpha\beta$ transgenic OT-II.2 (53) (purchased from Jackson Laboratory), and TCRβ transgenic (52) (generously provided by Karen Hathcock at National Institutes of Health, Baltimore, MD) mice were described previously and were maintained on a congenic C57BL/6J background. C57BL/6J inbred mice used for backcrossing and FVB/NJ mice were purchased from Jackson Laboratory. All mice were analyzed between 5 and 8 weeks of age. All mice used in this study were housed in the Unit for Laboratory Animal Medicine under specific-pathogen-free conditions, and all experiments were approved by the University Committee on the Use and Care of Animals at the University of Michigan.

Cell preparation and flow cytometry. Thymus, bone marrow, or spleen samples were dissected and then disrupted into single-cell suspensions by vigorous pipetting; the resulting suspensions were passed through a 40-μm cell strainer; and finally, the bone marrow or splenocyte cells were hemolyzed with ammonium chloride. Cells were first blocked for Fc receptors (FCRs) (anti-CD16/32; clone 2.4G2 [BD Pharmingen] or clone 93 [BioLegend]) and then stained with various combinations of antibodies (32, 74). Live cells were screened by forward and side scatter and propidium iodide (PI; Calbiochem), 4′,6-diamidino-2-phenylindole (DAPI; Roche), or Zombie fixable viability dye (BioLegend) exclusion. Cells were analyzed or sorted by flow cytometry (LSR Fortessa or FACSAria III; BD Biosciences). Sorted cells were reanalyzed to confirm that they were of >95% purity before subsequent analysis. Details of the antibodies used for flow cytometry are listed in Table 3. The negative-selection cocktail included anti-B220, -CD3, -CD8a, -CD11c, -CD19, -Gr1, -Mac-1, -NK1.1, -TCRβ, -TCR$\gamma\delta$, and -TER119 antibodies that were used to exclude mature hematopoietic-lineage cells (Lin^{+}) from immature thymocytes. Depending on specific experiments, CD8^{+} cells were removed prior to antibody staining by magnetic depletion (IMag; BD). Intracellular staining for the transcription factor GATA3 was performed by using the True-Nuclear Transcription Factor buffer set (BioLegend) with Zombie fixable viability dye (BioLegend), according to the manufacturer's instructions, after cell surface staining. Individual samples were divided into two portions after fixation and then incubated with equivalent amounts of anti-GATA3 antibody (16E10A23 [750 pg per million cells]; BioLegend) or an isotype control antibody (MPC-11 [750 pg per million cells]; BioLegend) for 45 to 60 min at room temperature. Data were analyzed by using FlowJo (Tree Star) or FACSDiva (BD Biosciences) software.

qRT-PCR analysis. Total RNA was isolated from sorted cells by using an RNeasy microkit (Qiagen) with DNase treatment and used to synthesize cDNA with a SuperScript III first-strand synthesis kit (Invitrogen). Reverse transcription-quantitative PCR was performed with SYBR green dye by using the StepOnePlus real-time PCR system (Applied Biosystems) as previously described (75). All qRT-PCR experiments were performed by using the total RT product from 100 cell equivalents, and results were quantified relative to the mRNA expression levels of the hypoxanthine phosphoribosyltransferase (HPRT) and β-actin endogenous reference genes. Primers used in this study included primers described

TABLE 3 Antibodies used for flow cytometry[c]

Manufacturer	Epitope	Clone	Fluorochrome for conjugation	Concn of antibody used per test (ng)
BD Pharmingen	TCR Vβ4	KT4	PE	500
	TCR Vβ5.1 5.2	MR9-4	FITC	400
	TCR Vβ8	F23.1	FITC	1,500
	TCR Vβ8	F23.1	PE	500
	TCR Vβ14	14-2	FITC	100
BioLegend	B220	RA3-6B2	FITC	50[a]
	CD3	17A2	FITC	50[a]
	CD3ε	145-2C11	APC	125
	CD4	RM4-5	PE-Cy7	125
	CD8a	53-6.7	Biotin	3.125 per million cells (for depletion)
	CD8a	53-6.7	FITC	50[a] (for lineage stain) 1,000 (for single stain)
	CD8a	53-6.7	APC	250
	CD8a	53-6.7	Brilliant Violet 510	25 per million cells
	CD11c	N418	FITC	12.5[a]
	CD19	6D5	FITC	12.5[a]
	CD25	PC61	PE-Cy7	25
	CD44	IM7	PerCP-Cy5.5	50
	CD62L	MEL-14	APC	25
	CD117 (cKit)	2B8	APC	25
	CD117 (cKit)	2B8	APC-Cy7	25
	GATA3	16E10A23	PE	0.75 per million cells
	Gr1	RB6-8C5	FITC	12.5[a]
	Mac1	M1/70	FITC	12.5[a]
	NK1.1	PK136	FITC	12.5[a]
	TER119	TER-119	FITC	50[a]
	TCRβ	H57-597	FITC	12.5[a]
	TCR Vα2	B20.1	FITC	50
	TCR Vα3.2	RR3-16	PE	50
	TCR Vα8.3	B21.14	PE	250
	TCR Vα11.1 11.2	RR8-1	PE	300
	TCR Vβ2	B20.6	PE	2,000
	TCR Vβ5.1 5.2	MR9-4	PE	125
	TCR Vβ6	RR4-7	PE	50
	TCR Vβ7	TR310	PE	125
	TCR Vβ9	MR10-2	PE	25
	TCR Vβ11	RR3-15	PE	100
	TCR Vβ12	MR11-1	PE	60
	TCR Vβ13	MR12-4	PE	200
	TCRγδ	GL3	FITC	12.5[a]
	Thy1.2	53-2.1	PerCP-Cy5.5	100
eBioscience	B220	RA3-6B2	eFluor 450	50[b]
	CD3	17A2	eFluor 450	50[b]
	CD3ε	145-2C11	eFluor 450	60
	CD8a	53-6.7	eFluor 450	12.5[b] (for lineage stain)
	CD11c	N418	eFluor 450	12.5[b]
	CD19	eBio1D3	eFluor 450	12.5[b]
	CD25	PC61.5	PerCP-Cy5.5	50
	CD27	LG.7F9	APC	25
	Gr1	RB6-8C5	eFluor 450	12.5[b]
	Mac1	M1/70	eFluor 450	12.5[b]
	NK1.1	PK136	eFluor 450	12.5[b]
	TER119	TER-119	eFluor 450	50[b]
	TCRβ	H57-597	eFluor 450	12.5[b]
	TCR Vβ10b	B21.5	PE	100
	TCRγδ	eBioGL3	eFluor 450	12.5[b]

[a]These antibody cocktails were used to exclude mature hematopoietic-lineage cells in thymocytes by conjugated fluorochrome FITC.

[b]These antibody cocktails were used to exclude mature hematopoietic-lineage cells in thymocytes by conjugated fluorochrome eFluor 450.

[c]Antibodies were titrated at six concentrations to determine the optimized usage prior to these experiments. Each test can be applied to as many as 15×10^6 cells in a 50- to 100-μl volume, unless otherwise noted. Isotype controls (if used) were used at the same amounts as the corresponding experimental antibody. PE, phycoerythrin; FITC, fluorescein isothiocyanate; APC, allophycocyanin; PerCP, peridinin chlorophyll protein.

TABLE 4 Primers used for analysis of *Tcrb* gene rearrangement

Primer	Sequence (5′→3′)	Reference[a]
Forward		
Vβ1	GTTGATTCGAAATGAGACGGTGCCC	25
Vβ2	GGAGTCCTGGGGACAAAGAGGTCA	
Vβ3	GAGGTGTATCCCTGAAAAGG	42
Vβ4	CCTGATATGCGAACAGTATCTAGGC	25
Vβ5	CCCAGCAGATTCTCAGTCCAACAG	25
Vβ6	GCGATCTATCTGAAGGCTATGATGC	25
Vβ7	GTACTGGTATCGACAAGACCC	42
Vβ8	GCATGGGCTGAGGCTGATCCATTA	25
Vβ9	GAACAGGGAAGCTGACAC	42
Vβ10	TCCAAGGCGCTTCTCACCTCAGTC	25
Vβ11	TGCTGGTGTCATCCAAACACCTAG	25
Vβ12	AGTTACCCAGACACCCAGACATGA	25
Vβ13	CTGCTGTGAGGCCTAAAGGAACTA	25
Vβ14	AGAGTCGGTGGTGCAACTGAACCT	25
Vβ15	CCCATCAGTCATCCCAACTTATCC	25
Vβ16	TAGGACAGCAGATGGAGTTTCTGG	25
Vβ17	GCACACTGCCTTTTACTGG	42
Vβ18	GGACATCTGTCAAAGTGGC	42
Vβ19	CTACAAGAAACCGGGAGAAGAACTC	26
Vβ20	GCCAGGAAGCAGAGATG	42
Dβ1	GCTTATCTGGTGGTTTCTTCCAGC	25
Dβ2	GTAGGCACCTGTGGGGAAGAAACT	25
β-actin F	GGCTGTATTCCCCTCCATCG	
β-actin F nested	TGGGGTTTTCTTGGGGATCG	
Reverse		
Jβ1 R	CAGAGAAGAGCAAGCGACCA	
Jβ2 R	TGAGAGCTGTCTCCTACTATCGATT	25
Jβ1 R nested	AAGGGACGACTCTGTCTTACCTTATACC	82
Jβ2 R nested	TTTCCCTCCCGGAGATTCCCTAA	25
β-actin R	CAATTGAGAAAGGGCGTGGC	

[a]Primers without a reference indicated were designed for this study.

previously for GATA3 (76), E47 (77), HPRT (78), and ACTB (79); forward primer 5′-CAAGGTAGCTTAGCCA ACATGG-3′ and reverse primer 5′-GTGGGTGTTGAATTTCATCGGG-3′ for RAG1; forward primer 5′-AGTAT TTCACATCCACAAGCAGG-3′ and reverse primer 5′-TGACCCACTGTTACCATCTGC-3′ for RAG2; forward primer 5′-GGGAATCTTCGACAGCCAGG-3′ and reverse primer 5′-AGTTTGAAGAGGAGCAGGCG-3′ for PTCRA; forward primer 5′-AGCAGCACTGTGTGCCCTGG-3′ and reverse primer 5′-TCTGGGTAGGTAGGGTT GGCTCC-3′ for ETS1; forward primer 5′-TTTTGGTGGGTGTTCTTGGC-3′ and reverse primer 5′-ACATTGCA TCAGAGACTTGGC-3′ for ATM; and forward primer 5′-GAGCCTCCTACTTCCAGTGC-3′ and reverse primer 5′-GAAGACATCCTCCTCGCAGC-3′ for CCND3.

RNA-seq analysis. Total RNA was isolated from sorted cells by using an RNeasy microkit (Qiagen) with DNase treatment. Intact total RNA with an RNA integrity value of >9.5 on an Agilent Bioanalyzer was further processed by using a Ribo-Zero Gold rRNA removal kit (Illumina) followed by library preparation. The library was sequenced (125-bp paired sequencing) on an Illumina HiSeq2000 instrument. Raw reads were mapped to the mm10 mouse reference genome sequence by using TopHat 2 (80) and further analyzed with Cufflinks and Cuffdiff (81). Data from three individual mice of the wild-type and $Tg^{Cd2\text{-}GATA3}$ genotypes were collected and compared. A default false discovery rate (FDR) of 0.05 was used to indicate statistical significance.

PCR analysis of *Tcrb* gene rearrangement in single cells. *Tcrb* gene rearrangement in single cells was analyzed by a seminested two-step PCR approach to amplify the *Tcrb* loci as described previously (25, 42), with modifications. In detail, after initial purification of DN4 stage T cells by flow sorting, single cells were resorted or isolated by using the CellCelector automated cell picking system (ALS Automated Lab Solutions GmbH, Jena, Germany); digested in a 20-μl solution containing 10 mM Tris-HCl (pH 9.0), 50 mM KCl, 1.5 mM $MgCl_2$, 3.0 μg proteinase K (EM Science), and 0.1% Triton X-100 (Sigma); and incubated at 55°C for 60 min followed by 95°C for 15 min. First-round PCR amplified both V(D)J-rearranged alleles together in a 60-μl final reaction mixture volume consisting of 20 μl of the single-cell isolation solution described above, PCR buffer (10 mM Tris-HCl [pH 9.0], 50 mM KCl, and 2.0 mM $MgCl_2$), 200 μM deoxynucleoside triphosphates (dNTPs), 0.5 U *Taq* DNA polymerase (New England BioLabs), and an oligonucleotide mixture (each at a 100 nM final concentration) (25, 26, 42, 82) (Table 4) containing 22 forward primers corresponding to 23 Vβ exon families (2 primers were designed to amplify 2 Vβ5 and 3 Vβ8 multisequence families, respectively), the Dβ1 and Dβ2 diversity segment genes, 2 reverse primers matching joining-segment Jβ1 and Jβ2 sequences, as well as 1 primer set for β-actin. The PCR conditions were 94°C for 1 min and 5 cycles with the annealing temperature ramped from 66°C to 58°C, followed by 25 cycles of 94°C for 30 s, 56°C for 60 s, and 72°C for 60 s, with a final extension step at 72°C for 5

min. A total of 1.0 μl of the first-round PCR product was used to perform seminested PCR with only β-actin primers to confirm the presence of a cell in each well and the efficiencies of single-cell sorting by flow cytometry, which overall were 65% ± 15% for live cells and 30% ± 15% for fixed cells; only β-actin-positive cells were analyzed by second-round PCRs (the conditions for β-actin amplification were 94°C for 1 min and 35 cycles of 94°C for 15 s, 60°C for 15 s, and 72°C for 30 s). Isolation of single cells by using the CellCelector system showed an average efficiency of 90%; the failure to select a single cell or the erroneous selection of 2 cells at the same time was monitored by imaging, ensuring the analysis of single cells exclusively.

For second-round PCRs, a total of 44 different primer sets were examined to determine which region was used for rearrangement in each cell. The second round of nested PCRs was performed by using 1.2 μl of the first-round PCR product, one forward primer (20 Vβ or 2 Dβ regions), one reverse primer (nested Jβ1 or Jβ2) (each at a 0.5 μM final concentration), PCR buffer, dNTPs, and 1.0 U of *Taq* DNA polymerase in a final reaction mixture volume of 20 μl. Amplification was carried out under the same conditions as those used for first-round PCR for 35 cycles. A total of 10 to 20% of the resulting PCR product was size fractionated on a 2% agarose gel, and positive bands from the VDJ amplification tube were then recovered and purified by using a GeneJET gel extraction kit (Fisher Scientific) and sequenced by using a specific Vβ forward primer on an Applied Biosystems 3730XL DNA sequencer at the University of Michigan Sequencing Core facility. If direct sequencing of any PCR product was ambiguous or exhibited sequence polymorphisms, these PCR products were subcloned and resequenced for verification. The purified PCR products were cloned by using a TOPO TA cloning kit (Invitrogen), individual clones were picked, and DNA was extracted by using a GeneJET Plasmid Miniprep kit (Fisher Scientific) and sequenced. The sequence was assessed for whether or not each rearrangement would predict a functional or defective gene product (VDJ^+ or VDJ^-) on the international ImMunoGeneTics information system website (http://www.imgt.org/). Sequences that did not correspond to a TCRβ gene or to an unrearranged TCRβ locus were probably recovered because of primer misannealing and were categorized as background and therefore removed from the frequency calculations.

Immunoblot analysis. Nuclear protein was extracted by using NE-PER nuclear and cytoplasmic extraction reagents (Thermo Scientific), and the protein concentration was determined by using a bicinchoninic acid (BCA) protein assay (Pierce, Thermo Scientific) according to the manufacturer's instructions. Totals of 10 μg and 5 μg of nuclear extracts were electrophoresed on a 4-to-15% gradient precast SDS-polyacrylamide gel (Bio-Rad), transferred to a nitrocellulose membrane (Li-Cor), and first blotted by using a rabbit anti-GATA3 antibody (clone 11599 [32]). Anti-GATA3 immunoreactivity was then detected by using a fluorescently labeled donkey anti-rabbit secondary antibody (IRDye; Li-Cor) and quantified by using the Odyssey infrared imaging system (Li-Cor Bioscience). Anti-lamin B (M-20; Santa Cruz) was used as the internal control.

Statistical analysis. Statistical significance was determined by the Student *t* test. Data were considered statistically significant when the *P* value was <0.05. Fisher's exact tests were performed for the *Tcrb* genomic configuration data in Table 1, and data were considered statistically different when the *P* value was <0.05.

ACKNOWLEDGMENTS

This work was supported by National Institutes of Health grants AI094642 (T.H. and J.D.E.), AI063058 (J.M.S.), AI091627 (I.M.), and NSF1452656 (Y.G.). The research was also supported in part by a University of Michigan Comprehensive Cancer Center support grant (P30 CA046592) that provides support for the Flow Cytometry and DNA Sequencing Core facilities at the University of Michigan.

We are grateful to Constantin Nelep for assistance using the CellCelector (ALS Automated Lab Solutions GmbH, Jena, Germany) to isolate single cells.

We declare that we have no competing financial interests.

C.-J.K. designed the study, performed experiments, analyzed the data, and wrote the manuscript. B.P. and Y.G. analyzed RNA-seq data. S.T. and K.Y. contributed GATA3 transgenic mouse lines and edited the manuscript. J.M.S. and I.M. designed the study and edited the manuscript. T.H. and J.D.E. designed the study, analyzed the data, and wrote the manuscript.

REFERENCES

1. Cedar H, Bergman Y. 2008. Choreography of Ig allelic exclusion. Curr Opin Immunol 20:308–317. https://doi.org/10.1016/j.coi.2008.02.002.
2. Mostoslavsky R, Alt FW, Rajewsky K. 2004. The lingering enigma of the allelic exclusion mechanism. Cell 118:539–544. https://doi.org/10.1016/j.cell.2004.08.023.
3. Tonegawa S. 1983. Somatic generation of antibody diversity. Nature 302:575–581. https://doi.org/10.1038/302575a0.
4. Burnet FM. 1959. The clonal selection theory of acquired immunity. Vanderbilt University Press, Nashville, TN.
5. Anderson G, Jenkinson EJ. 2001. Lymphostromal interactions in thymic development and function. Nat Rev Immunol 1:31–40. https://doi.org/10.1038/35095500.
6. Allman D, Sambandam A, Kim S, Miller JP, Pagan A, Well D, Meraz A, Bhandoola A. 2003. Thymopoiesis independent of common lymphoid progenitors. Nat Immunol 4:168–174. https://doi.org/10.1038/ni878.
7. Porritt HE, Rumfelt LL, Tabrizifard S, Schmitt TM, Zuniga-Pflucker JC, Petrie HT. 2004. Heterogeneity among DN1 prothymocytes reveals multiple progenitors with different capacities to generate T cell and non-T

cell lineages. Immunity 20:735–745. https://doi.org/10.1016/j.immuni.2004.05.004.
8. Sambandam A, Maillard I, Zediak VP, Xu L, Gerstein RM, Aster JC, Pear WS, Bhandoola A. 2005. Notch signaling controls the generation and differentiation of early T lineage progenitors. Nat Immunol 6:663–670. https://doi.org/10.1038/ni1216.
9. Tan JB, Visan I, Yuan JS, Guidos CJ. 2005. Requirement for Notch1 signals at sequential early stages of intrathymic T cell development. Nat Immunol 6:671–679. https://doi.org/10.1038/ni1217.
10. Bell JJ, Bhandoola A. 2008. The earliest thymic progenitors for T cells possess myeloid lineage potential. Nature 452:764–767. https://doi.org/10.1038/nature06840.
11. Fowlkes BJ, Edison L, Mathieson BJ, Chused TM. 1985. Early T lymphocytes Differentiation in vivo of adult intrathymic precursor cells. J Exp Med 162:802–822. https://doi.org/10.1084/jem.162.3.802.
12. Rothenberg EV, Zhang J, Li L. 2010. Multilayered specification of the T-cell lineage fate. Immunol Rev 238:150–168. https://doi.org/10.1111/j.1600-065X.2010.00964.x.
13. Rothenberg EV. 2011. T cell lineage commitment: identity and renunciation. J Immunol 186:6649–6655. https://doi.org/10.4049/jimmunol.1003703.
14. Krangel MS. 2009. Mechanics of T cell receptor gene rearrangement. Curr Opin Immunol 21:133–139. https://doi.org/10.1016/j.coi.2009.03.009.
15. Scott CS, Richards SJ, Roberts BE. 1990. Patterns of membrane TcR alpha beta and TcR gamma delta chain expression by normal blood $CD4^+$ $CD8^-$, $CD4^-$ $CD8^+$, $CD4^-$ $CD8^{dim+}$ and $CD4^-$ $CD8^-$ lymphocytes. Immunology 70:351–356.
16. Morris GP, Allen PM. 2012. How the TCR balances sensitivity and specificity for the recognition of self and pathogens. Nat Immunol 13:121–128. https://doi.org/10.1038/ni.2190.
17. Gerby B, Tremblay CS, Tremblay M, Rojas-Sutterlin S, Herblot S, Hebert J, Sauvageau G, Lemieux S, Lecuyer E, Veiga DF, Hoang T. 2014. SCL, LMO1 and Notch1 reprogram thymocytes into self-renewing cells. PLoS Genet 10:e1004768. https://doi.org/10.1371/journal.pgen.1004768.
18. Godfrey DI, Kennedy J, Mombaerts P, Tonegawa S, Zlotnik A. 1994. Onset of TCR-beta gene rearrangement and role of TCR-beta expression during $CD3^-$ $CD4^-$ $CD8^-$ thymocyte differentiation. J Immunol 152:4783–4792.
19. Hu J, Zhang Y, Zhao L, Frock RL, Du Z, Meyers RM, Meng FL, Schatz DG, Alt FW. 2015. Chromosomal loop domains direct the recombination of antigen receptor genes. Cell 163:947–959. https://doi.org/10.1016/j.cell.2015.10.016.
20. Mombaerts P, Clarke AR, Rudnicki MA, Iacomini J, Itohara S, Lafaille JJ, Wang L, Ichikawa Y, Jaenisch R, Hooper ML, Tonegawa S. 1992. Mutations in T-cell antigen receptor genes alpha and beta block thymocyte development at different stages. Nature 360:225–231. https://doi.org/10.1038/360225a0.
21. Shinkai Y, Rathbun G, Lam KP, Oltz EM, Stewart V, Mendelsohn M, Charron J, Datta M, Young F, Stall AM, Alt FW. 1992. RAG-2-deficient mice lack mature lymphocytes owing to inability to initiate V(D)J rearrangement. Cell 68:855–867. https://doi.org/10.1016/0092-8674(92)90029-C.
22. Yancopoulos GD, Alt FW. 1986. Regulation of the assembly and expression of variable-region genes. Annu Rev Immunol 4:339–368. https://doi.org/10.1146/annurev.iy.04.040186.002011.
23. Bergman Y. 1999. Allelic exclusion in B and T lymphopoiesis. Semin Immunol 11:319–328. https://doi.org/10.1006/smim.1999.0188.
24. Malissen M, Trucy J, Jouvin-Marche E, Cazenave PA, Scollay R, Malissen B. 1992. Regulation of TCR alpha and beta gene allelic exclusion during T-cell development. Immunol Today 13:315–322. https://doi.org/10.1016/0167-5699(92)90044-8.
25. Aifantis I, Buer J, von Boehmer H, Azogui O. 1997. Essential role of the pre-T cell receptor in allelic exclusion of the T cell receptor β locus. Immunity 7:601–607. https://doi.org/10.1016/S1074-7613(00)80381-7.
26. Gartner F, Alt FW, Monroe R, Chu M, Sleckman BP, Davidson L, Swat W. 1999. Immature thymocytes employ distinct signaling pathways for allelic exclusion versus differentiation and expansion. Immunity 10:537–546. https://doi.org/10.1016/S1074-7613(00)80053-9.
27. Hinz T, Weidmann E, Kabelitz D. 2001. Dual TCR-expressing T lymphocytes in health and disease. Int Arch Allergy Immunol 125:16–20. https://doi.org/10.1159/000053792.
28. Auger JL, Haasken S, Steinert EM, Binstadt BA. 2012. Incomplete TCR-beta allelic exclusion accelerates spontaneous autoimmune arthritis in K/BxN TCR transgenic mice. Eur J Immunol 42:2354–2362. https://doi.org/10.1002/eji.201242520.
29. Yamamoto M, Ko LJ, Leonard MW, Beug H, Orkin SH, Engel JD. 1990. Activity and tissue-specific expression of the transcription factor NF-E1 multigene family. Genes Dev 4:1650–1662. https://doi.org/10.1101/gad.4.10.1650.
30. Ko LJ, Yamamoto M, Leonard MW, George KM, Ting P, Engel JD. 1991. Murine and human T-lymphocyte GATA-3 factors mediate transcription through a cis-regulatory element within the human T-cell receptor delta gene enhancer. Mol Cell Biol 11:2778–2784. https://doi.org/10.1128/MCB.11.5.2778.
31. Hosoya T, Maillard I, Engel JD. 2010. From the cradle to the grave: activities of GATA-3 throughout T-cell development and differentiation. Immunol Rev 238:110–125. https://doi.org/10.1111/j.1600-065X.2010.00954.x.
32. Hosoya T, Kuroha T, Moriguchi T, Cummings D, Maillard I, Lim K-C, Engel JD. 2009. GATA-3 is required for early T lineage progenitor development. J Exp Med 206:2987–3000. https://doi.org/10.1084/jem.20090934.
33. Scripture-Adams DD, Damle SS, Li L, Elihu KJ, Qin S, Arias AM, Butler RR, Champhekar A, Zhang JA, Rothenberg EV. 2014. GATA-3 dose-dependent checkpoints in early T cell commitment. J Immunol 193:3470–3491. https://doi.org/10.4049/jimmunol.1301663.
34. Pai S-Y, Truitt ML, Ting C-N, Leiden JM, Glimcher LH, Ho I-C. 2003. Critical roles for transcription factor GATA-3 in thymocyte development. Immunity 19:863–875. https://doi.org/10.1016/S1074-7613(03)00328-5.
35. Wang L, Wildt KF, Zhu J, Zhang X, Feigenbaum L, Tessarollo L, Paul WE, Fowlkes BJ, Bosselut R. 2008. Distinct functions for the transcription factors GATA-3 and ThPOK during intrathymic differentiation of CD4(+) T cells. Nat Immunol 9:1122–1130. https://doi.org/10.1038/ni.1647.
36. Yoh K, Shibuya K, Morito N, Nakano T, Ishizaki K, Shimohata H, Nose M, Izui S, Shibuya A, Koyama A, Engel JD, Yamamoto M, Takahashi S. 2003. Transgenic overexpression of GATA-3 in T lymphocytes improves autoimmune glomerulonephritis in mice with a BXSB/MpJ-Yaa genetic background. J Am Soc Nephrol 14:2494–2502. https://doi.org/10.1097/01.ASN.0000086473.23379.25.
37. Zhumabekov T, Corbella P, Tolaini M, Kioussis D. 1995. Improved version of a human CD2 minigene based vector for T cell-specific expression in transgenic mice. J Immunol Methods 185:133–140. https://doi.org/10.1016/0022-1759(95)00124-S.
38. de Boer J, Williams A, Skavdis G, Harker N, Coles M, Tolaini M, Norton T, Williams K, Roderick K, Potocnik AJ, Kioussis D. 2003. Transgenic mice with hematopoietic and lymphoid specific expression of Cre. Eur J Immunol 33:314–325. https://doi.org/10.1002/immu.200310005.
39. Taghon T, Yui MA, Pant R, Diamond RA, Rothenberg EV. 2006. Developmental and molecular characterization of emerging beta- and gammadelta-selected pre-T cells in the adult mouse thymus. Immunity 24:53–64. https://doi.org/10.1016/j.immuni.2005.11.012.
40. Taghon T, Yui MA, Rothenberg EV. 2007. Mast cell lineage diversion of T lineage precursors by the essential T cell transcription factor GATA-3. Nat Immunol 8:845–855. https://doi.org/10.1038/ni1486.
41. Huang DW, Sherman BT, Lempicki RA. 2009. Systematic and integrative analysis of large gene lists using DAVID bioinformatics resources. Nat Protoc 4:44–57. https://doi.org/10.1038/nprot.2008.211.
42. Dash P, McClaren JL, Oguin TH, III, Rothwell W, Todd B, Morris MY, Becksfort J, Reynolds C, Brown SA, Doherty PC, Thomas PG. 2011. Paired analysis of TCRalpha and TCRbeta chains at the single-cell level in mice. J Clin Invest 121:288–295. https://doi.org/10.1172/JCI44752.
43. Balomenos D, Balderas RS, Mulvany KP, Kaye J, Kono DH, Theofilopoulos AN. 1995. Incomplete T cell receptor V beta allelic exclusion and dual V beta-expressing cells. J Immunol 155:3308–3312.
44. ten Boekel E, Melchers F, Rolink A. 1995. The status of Ig loci rearrangements in single cells from different stages of B cell development. Int Immunol 7:1013–1019. https://doi.org/10.1093/intimm/7.6.1013.
45. ten Boekel E, Melchers F, Rolink AG. 1998. Precursor B cells showing H chain allelic inclusion display allelic exclusion at the level of pre-B cell receptor surface expression. Immunity 8:199–207. https://doi.org/10.1016/S1074-7613(00)80472-0.
46. Eyquem S, Chemin K, Fasseu M, Bories JC. 2004. The Ets-1 transcription factor is required for complete pre-T cell receptor function and allelic exclusion at the T cell receptor beta locus. Proc Natl Acad Sci U S A 101:15712–15717. https://doi.org/10.1073/pnas.0405546101.
47. Steinel NC, Fisher MR, Yang-Iott KS, Bassing CH. 2014. The ataxia telangiectasia mutated and cyclin D3 proteins cooperate to help enforce

TCRbeta and IgH allelic exclusion. J Immunol 193:2881–2890. https://doi.org/10.4049/jimmunol.1302201.
48. Alam SM, Gascoigne NR. 1998. Posttranslational regulation of TCR Valpha allelic exclusion during T cell differentiation. J Immunol 160:3883–3890.
49. Ku CJ, Lim KC, Kalantry S, Maillard I, Engel JD, Hosoya T. 2015. A monoallelic-to-biallelic T-cell transcriptional switch regulates GATA3 abundance. Genes Dev 29:1930–1941. https://doi.org/10.1101/gad.265025.115.
50. Moriguchi T, Yu L, Otsuki A, Ainoya K, Lim KC, Yamamoto M, Engel JD. 13 June 2016. Gata3 hypomorphic mutant mice rescued with a YAC transgene suffer a glomerular mesangial cell defect. Mol Cell Biol https://doi.org/10.1128/MCB.00173-16.
51. Uematsu Y, Ryser S, Dembić Z, Borgulya P, Krimpenfort P, Berns A, von Boehmer H, Steinmetz M. 1988. In transgenic mice the introduced functional T cell receptor β gene prevents expression of endogenous β genes. Cell 52:831–841. https://doi.org/10.1016/0092-8674(88)90425-4.
52. Shinkai Y, Koyasu S, Nakayama K, Murphy KM, Loh DY, Reinherz EL, Alt FW. 1993. Restoration of T cell development in RAG-2-deficient mice by functional TCR transgenes. Science 259:822–825. https://doi.org/10.1126/science.8430336.
53. Barnden MJ, Allison J, Heath WR, Carbone FR. 1998. Defective TCR expression in transgenic mice constructed using cDNA-based α- and β-chain genes under the control of heterologous regulatory elements. Immunol Cell Biol 76:34–40. https://doi.org/10.1046/j.1440-1711.1998.00709.x.
54. Oettinger MA, Schatz DG, Gorka C, Baltimore D. 1990. RAG-1 and RAG-2, adjacent genes that synergistically activate V(D)J recombination. Science 248:1517–1523. https://doi.org/10.1126/science.2360047.
55. Agata Y, Tamaki N, Sakamoto S, Ikawa T, Masuda K, Kawamoto H, Murre C. 2007. Regulation of T cell receptor beta gene rearrangements and allelic exclusion by the helix-loop-helix protein, E47. Immunity 27:871–884. https://doi.org/10.1016/j.immuni.2007.11.015.
56. Kim S, Davis M, Sinn E, Patten P, Hood L. 1981. Antibody diversity: somatic hypermutation of rearranged VH genes. Cell 27:573–581. https://doi.org/10.1016/0092-8674(81)90399-8.
57. Ko LJ, Engel JD. 1993. DNA-binding specificities of the GATA transcription factor family. Mol Cell Biol 13:4011–4022. https://doi.org/10.1128/MCB.13.7.4011.
58. Wei G, Abraham BJ, Yagi R, Jothi R, Cui K, Sharma S, Narlikar L, Northrup DL, Tang Q, Paul WE, Zhu J, Zhao K. 2011. Genome-wide analyses of transcription factor GATA3-mediated gene regulation in distinct T cell types. Immunity 35:299–311. https://doi.org/10.1016/j.immuni.2011.08.007.
59. Joulin V, Bories D, Eléouet JF, Labastie MC, Chrétien S, Mattéi MG, Roméo PH. 1991. A T-cell specific TCR delta DNA binding protein is a member of the human GATA family. EMBO J 10:1809–1816.
60. Ho IC, Vorhees P, Marin N, Oakley BK, Tsai SF, Orkin SH, Leiden JM. 1991. Human GATA-3: a lineage-restricted transcription factor that regulates the expression of the T cell receptor alpha gene. EMBO J 10:1187–1192.
61. Kurek D, Garinis GA, van Doorninck JH, van der Wees J, Grosveld FG. 2007. Transcriptome and phenotypic analysis reveals Gata3-dependent signalling pathways in murine hair follicles. Development 134:261–272. https://doi.org/10.1242/dev.02721.
62. Yang Z, Gu L, Romeo PH, Bories D, Motohashi H, Yamamoto M, Engel JD. 1994. Human GATA-3 trans-activation, DNA-binding, and nuclear localization activities are organized into distinct structural domains. Mol Cell Biol 14:2201–2212. https://doi.org/10.1128/MCB.14.3.2201.
63. Moriguchi T, Takako N, Hamada M, Maeda A, Fujioka Y, Kuroha T, Huber RE, Hasegawa SL, Rao A, Yamamoto M, Takahashi S, Lim KC, Engel JD. 2006. Gata3 participates in a complex transcriptional feedback network to regulate sympathoadrenal differentiation. Development 133:3871–3881. https://doi.org/10.1242/dev.02553.
64. Proudhon C, Hao B, Raviram R, Chaumeil J, Skok JA. 2015. Long-range regulation of V(D)J recombination. Adv Immunol 128:123–182. https://doi.org/10.1016/bs.ai.2015.07.003.
65. Porcher C, Liao EC, Fujiwara Y, Zon LI, Orkin SH. 1999. Specification of hematopoietic and vascular development by the bHLH transcription factor SCL without direct DNA binding. Development 126:4603–4615.
66. Wright CW, Duckett CS. 2009. The aryl hydrocarbon nuclear translocator alters CD30-mediated NF-kappaB-dependent transcription. Science 323:251–255. https://doi.org/10.1126/science.1162818.
67. Motohashi H, Katsuoka F, Shavit JA, Engel JD, Yamamoto M. 2000. Positive or negative MARE-dependent transcriptional regulation is determined by the abundance of small Maf proteins. Cell 103:865–875. https://doi.org/10.1016/S0092-8674(00)00190-2.
68. Ting CN, Olson MC, Barton KP, Leiden JM. 1996. Transcription factor GATA-3 is required for development of the T-cell lineage. Nature 384:474–478. https://doi.org/10.1038/384474a0.
69. Anderson MK, Hernandez-Hoyos G, Dionne CJ, Arias AM, Chen D, Rothenberg EV. 2002. Definition of regulatory network elements for T cell development by perturbation analysis with PU.1 and GATA-3. Dev Biol 246:103–121. https://doi.org/10.1006/dbio.2002.0674.
70. Van Esch H, Groenen P, Nesbit MA, Schuffenhauer S, Lichtner P, Vanderlinden G, Harding B, Beetz R, Bilous RW, Holdaway I, Shaw NJ, Fryns JP, Van de Ven W, Thakker RV, Devriendt K. 2000. GATA3 haplo-insufficiency causes human HDR syndrome. Nature 406:419–422. https://doi.org/10.1038/35019088.
71. Daw SC, Taylor C, Kraman M, Call K, Mao J, Schuffenhauer S, Meitinger T, Lipson T, Goodship J, Scambler P. 1996. A common region of 10p deleted in DiGeorge and velocardiofacial syndromes. Nat Genet 13:458–460. https://doi.org/10.1038/ng0896-458.
72. Lichtner P, Konig R, Hasegawa T, Van Esch H, Meitinger T, Schuffenhauer S. 2000. An HDR (hypoparathyroidism, deafness, renal dysplasia) syndrome locus maps distal to the DiGeorge syndrome region on 10p13/14. J Med Genet 37:33–37. https://doi.org/10.1136/jmg.37.1.33.
73. Nawijn MC, Ferreira R, Dingjan GM, Kahre O, Drabek D, Karis A, Grosveld F, Hendriks RW. 2001. Enforced expression of GATA-3 during T cell development inhibits maturation of CD8 single-positive cells and induces thymic lymphoma in transgenic mice. J Immunol 167:715–723. https://doi.org/10.4049/jimmunol.167.2.715.
74. Maillard I, Schwarz BA, Sambandam A, Fang T, Shestova O, Xu L, Bhandoola A, Pear WS. 2006. Notch-dependent T-lineage commitment occurs at extrathymic sites following bone marrow transplantation. Blood 107:3511–3519. https://doi.org/10.1182/blood-2005-08-3454.
75. Ku CJ, Hosoya T, Maillard I, Engel JD. 2012. GATA-3 regulates hematopoietic stem cell maintenance and cell-cycle entry. Blood 119:2242–2251. https://doi.org/10.1182/blood-2011-07-366070.
76. Yu Q, Sharma A, Oh SY, Moon H-G, Hossain MZ, Salay TM, Leeds KE, Du H, Wu B, Waterman ML, Zhu Z, Sen JM. 2009. T cell factor 1 initiates the T helper type 2 fate by inducing the transcription factor GATA-3 and repressing interferon-γ. Nat Immunol 10:992–999. https://doi.org/10.1038/ni.1762.
77. Li L, Jothi R, Cui K, Lee JY, Cohen T, Gorivodsky M, Tzchori I, Zhao Y, Hayes SM, Bresnick EH, Zhao K, Westphal H, Love PE. 2011. Nuclear adaptor Ldb1 regulates a transcriptional program essential for the maintenance of hematopoietic stem cells. Nat Immunol 12:129–136. https://doi.org/10.1038/ni.1978.
78. Maillard I, Koch U, Dumortier A, Shestova O, Xu L, Sai H, Pross SE, Aster JC, Bhandoola A, Radtke F, Pear WS. 2008. Canonical Notch signaling is dispensable for the maintenance of adult hematopoietic stem cells. Cell Stem Cell 2:356–366. https://doi.org/10.1016/j.stem.2008.02.011.
79. Esteghamat F, Gillemans N, Bilic I, van Den Akker E, Cantù I, van Gent T, Klingmüller U, van Lom K, von Lindern M, Grosveld F, Bryn van Dijk T, Busslinger M, Philipsen S. 2013. Erythropoiesis and globin switching in compound Klf1::Bcl11a mutant mice. Blood 121:2553–2562. https://doi.org/10.1182/blood-2012-06-434530.
80. Kim D, Pertea G, Trapnell C, Pimentel H, Kelley R, Salzberg SL. 2013. TopHat2: accurate alignment of transcriptomes in the presence of insertions, deletions and gene fusions. Genome Biol 14:R36. https://doi.org/10.1186/gb-2013-14-4-r36.
81. Trapnell C, Roberts A, Goff L, Pertea G, Kim D, Kelley DR, Pimentel H, Salzberg SL, Rinn JL, Pachter L. 2012. Differential gene and transcript expression analysis of RNA-seq experiments with TopHat and Cufflinks. Nat Protoc 7:562–578. https://doi.org/10.1038/nprot.2012.016.
82. Giblin W, Chatterji M, Westfield G, Masud T, Theisen B, Cheng HL, DeVido J, Alt FW, Ferguson DO, Schatz DG, Sekiguchi J. 2009. Leaky severe combined immunodeficiency and aberrant DNA rearrangements due to a hypomorphic RAG1 mutation. Blood 113:2965–2975. https://doi.org/10.1182/blood-2008-07-165167.
83. Krimpenfort P, de Jong R, Uematsu Y, Dembic Z, Ryser S, von Boehmer H, Steinmetz M, Berns A. 1988. Transcription of T cell receptor beta-chain genes is controlled by a downstream regulatory element. EMBO J 7:745–750.